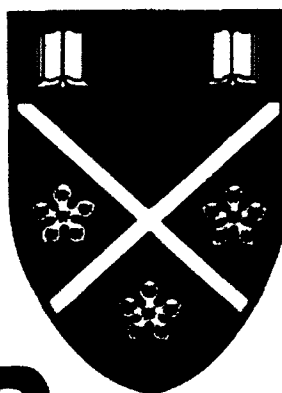




# UNIVERSITY OF STRATHCLYDE



SDTIC  
ELECTE  
JUN 28 1993  
A D

## INVESTIGATION OF A FIBRE OPTIC FREQUENCY SHIFTER AND OPTICAL ISOLATOR

This document has been approved  
for public release and sale; its  
distribution is unlimited.

AFOSR 90-0286

FINAL REPORT - 30 APRIL 1993



**INVESTIGATION OF A FIBRE OPTIC  
FREQUENCY SHIFTER  
AND OPTICAL ISOLATOR**

**AFOSR 90-0286**

**FINAL REPORT - 30 APRIL 1993**

*W Johnstone, G Thursby and C Michie  
University of Strathclyde  
Electronic & Electrical Engineering Department  
Royal College Building  
204 George Street  
Glasgow G1 1XW*

# REPORT DOCUMENTATION PAGE

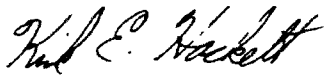
Form Approved  
OMB No. 0704-0188

Public reporting burden for this collection of information is estimated to average 1 hour per response, including the time for reviewing instructions, searching existing data sources, gathering and maintaining the data needed, and completing and reviewing the collection of information. Send comments regarding this burden estimate or any other aspect of this collection of information, including suggestions for reducing this burden, to Washington Headquarters Services, Directorate for Information Operations and Reports, 1215 Jefferson Davis Highway, Suite 1204, Arlington, VA 22202-4302, and to the Office of Management and Budget, Paperwork Reduction Project (0704-0188), Washington, DC 20503.

1. AGENCY USE ONLY (Leave blank)		2. REPORT DATE 30/4/93		3. REPORT TYPE AND DATES COVERED Final 30/9/90 - 30/4/93	
4. TITLE AND SUBTITLE A Fibre Optic Frequency Shifter and Optical Isolator				5. FUNDING NUMBERS AFOSR-90-0286	
6. AUTHOR(S) Dr Walter Johnstone Dr Graham Thursby Dr Craig Michie					
7. PERFORMING ORGANIZATION NAME(S) AND ADDRESS(ES) University of Strathclyde Department of Electronic & Electrical Engineering 204 George Street Glasgow G1 1XW, Scotland United Kingdom				8. PERFORMING ORGANIZATION REPORT NUMBER A1	
9. SPONSORING/MONITORING AGENCY NAME(S) AND ADDRESS(ES) European Office of Aerospace Research and Development PSC 802 Box 14 FPO AE 09499-0200				10. SPONSORING/MONITORING AGENCY REPORT NUMBER EOARD 93-06	
11. SUPPLEMENTARY NOTES					
12a. DISTRIBUTION/AVAILABILITY STATEMENT Approved for public release Distribution unlimited				12b. DISTRIBUTION CODE	
13. ABSTRACT (Maximum 200 words)  This report documents a programme of investigation of an in line fibre optic frequency translator and optical isolator on behalf of AFOSR (90-0286). The proposed designs are based on evanescent field coupling from a single mode optical fibre to a multi-mode planar waveguide overlay. The programme focused mainly on the development of a particular design of frequency translator and included extensive characterisation of fibre optic overlay structures in general. Fabrication of the frequency translator based on bonding lithium niobate to a fibre block and polishing it thin to form the acousto optic overlay proved to be difficult and yields were low. Several devices were completed but frequency shifting was not observed due to severe attenuation of the surface acoustic waves. On a more positive note the overlay structures demonstrated excellent wavelength selective properties leading to the realisation of tunable high resolution (2nm) dropping filters and band pass filters. Such devices have many applications in communications, sensing and tuning of fibre lasers.					
14. SUBJECT TERMS Fibre Optic Components Frequency Translators Optical Isolator				15. NUMBER OF PAGES 30	
				16. PRICE CODE	
17. SECURITY CLASSIFICATION OF REPORT UNCLASSIFIED	18. SECURITY CLASSIFICATION OF THIS PAGE UNCLASSIFIED	19. SECURITY CLASSIFICATION OF ABSTRACT UNCLASSIFIED	20. LIMITATION OF ABSTRACT		

This report has been reviewed and is releasable to the National Technical Information Service (NTIS).  
At NTIS it will be releasable to the general public, including foreign nations.

This technical report has been reviewed and is approved for publication.

  
fa PARRIS C. NEAL, Lt Col, USAF  
Chief, Aerospace Electronics

  
RONALD J. LISOWSKI, Lt Col, USAF  
Chief Scientist

# CONTENTS

<b>1. Introduction</b>	<b>3</b>
<b>2. Preliminary Investigation of Fibre Optic Overlay Devices</b>	<b>7</b>
2.1 Basic Theory	7
2.2 Resonance Spacing	8
2.3 Index and Wavelength Response	8
2.4 Resonance Linewidth	9
2.5 Conclusion	10
<b>3. All Solid State Fibre Optic Overlay Devices</b>	<b>11</b>
3.1 Device Fabrication	11
3.2 Zinc Sulphide, Zinc Selenide and Glass Overlay Devices	12
3.3 Lithium Niobate Overlay Devices	14
3.4 Magnetic Optic Overlay Devices	15
<b>4. Acousto-Optic Frequency Shifter: Design Considerations</b>	<b>16</b>
4.1 Evanescently Coupled Bragg Frequency Shifter	16
4.2 Acousto-Optic Frequency Shifter: Modulation of Coupling to the Overlay	18
4.3 Fibre Mode Coupled Frequency Shifter	20
<b>5. Optical Isolator Design</b>	<b>21</b>
<b>6. Fabrication of the Frequency Translator</b>	<b>23</b>
6.1 Production of Side Polished Fibre Blocks	23
6.2 Fabrication of the Multimode Overlay Waveguide	24
6.3 Fabrication of the SAW Interdigital Electrode Structure	28

<b>7. Frequency Shifter Testing</b>	<b>32</b>
<b>8. Wavelength Selective Elements</b>	<b>36</b>
<b>9. Conclusions</b>	<b>37</b>
<b>References</b>	<b>39</b>
<b>Figures</b>	

Accession For	
NTIS - GRA&I	<input checked="" type="checkbox"/>
DTIC TAB	<input type="checkbox"/>
Unannounced	<input type="checkbox"/>
Justification	
By	
Distribution /	
Availability Codes	
Dist	Avail. and/or Special
A-1	

DTIC QUALITY INSPECTED 2

## INVESTIGATION OF A FIBRE OPTIC FREQUENCY SHIFTER AND OPTICAL ISOLATER

### SUMMARY

At Strathclyde, evanescent field optical coupling from a side polished optical fibre to a solid state multi-mode waveguide overlay had been shown to exhibit a useful wavelength selective response. In addition some progress had been made towards the use of electro optic materials such as lithium niobate in the role of the overlay to achieve wavelength tuning and/or modulation. The lithium niobate was bonded to a polished fibre block and then polished to the required thickness ( $< 30\mu\text{m}$ ). Following a request from AFOSR in 1990, Strathclyde proposed a programme to investigate the use of such a structure in the realisation of an in line frequency translator (using surface acoustic waves, SAWs, launched by an interdigital electrode structure) and an optical isolator. The main perceived advantage is that the fibre remains continuous in this structure, obviating the problems of fibre to device interfacing associated with other technologies such as integrated optics.

The executed programme focused mainly on the fabrication of one particular design of frequency translator and incorporated the development and characterisation of fibre optic overlay devices in general. Fabrication difficulties associated with overlay disintegration during polishing or during the harsh processes involved in interdigital electrode formation led to low yields of complete frequency translation structures. Indeed, many weeks of painstaking effort by highly skilled personnel were required to fabricate a single device. Several completed devices were realised over the last nine months of the project (including the six months extension period). However, despite exhaustive testing, frequency translation has not been observed. Further testing has demonstrated that the acoustic waves are severely attenuated by the  $1\mu\text{m}$  thick adhesive layer which bonds the lithium niobate to the polished fibre block. In view of this it was concluded that devices fabricated by the bonding/polishing approach adopted here would have very low efficiency and would not lend themselves to ease of manufacture. Any further investigation of this basic frequency shifting structure should use vacuum deposited active overlays of PLZT or ZnO.

In the course of the frequency shifter development programme considerable progress was made on the development and characterisation of fibre optic overlay devices as

wavelength selective elements and high resolution (down to a few nanometers) has been achieved in both a channel drop and band pass configurations. In addition, the principle of tuning by variation of the refractive index of the superstrate or overlay (e.g. electro optically) has been demonstrated. Such devices have extensive applications in fibre optic technology including wavelength division multiplexing, filtering (e.g. of optically amplified signals), optical sensing (e.g. pH, chemical and environmental sensing) and in the tuning of fibre lasers. The latter is rapidly growing in interest and outwith the present programme we have used a bandpass structure based on the above technology in an erbium doped fibre ring laser to provide single mode operation ( $\sim 100\text{kHz}$  linewidth) tunable over the entire erbium gain curve.

As regards the optical isolator several attempts were made to realise a device. However, severe material handling problems precluded the achievement of anything useful in terms of the original design. Work on the isolator was eventually terminated by mutual agreement with the project monitor (see quarterly report May 1992).

At Strathclyde we believe that there is no fundamental reason for the failure to observe frequency translation in the proposed structure. We also believe that such a device would be an important contribution to the optical engineering community. It is intended, therefore, that we will continue this work towards the realisation of a frequency translator and we will inform AFOSR of any significant progress.

## 1. INTRODUCTION

The recent growth in the use of optical fibres in telecommunications, sensing, and signal processing has placed ever increasing demands on the supply of novel, rugged, in-line components. To avoid the fibre to device interfacing problems of integrated or micro-optic component technology, device architectures which offer an active or passive function without interruption of the fibre are of great interest to the optical engineering community. Recently, such a device structure, involving evanescent coupling from an optical fibre, side-polished close to the core, to a planar multimode waveguide overlay, has been investigated at Strathclyde University for the realisation of wavelength selective elements, modulators and switches. The aims of this particular project were to develop an in-line frequency translator and optical isolator based on this device structure offering considerable advantages in terms of mechanical reliability, compactness, loss and fibre interfacing.

The basic structure<sup>1</sup> of the proposed components comprises a high index ( $>$ the fibre core index) multimode, planar, waveguide overlay evanescently coupled to the optical field in a side-polished single mode optical fibre<sup>2</sup> (Fig.1). The modes of the overlay range in effective index ( $n_{eo}$ ) from that of the fundamental, just less than the material index ( $n_o$ ), to that of the highest order mode just greater than the fibre cladding index ( $n_1$ ). For a particular overlay  $V$  number the highest order mode, close to cut off, can be made to match the effective index of the fibre core ( $n_{ef}$ ) resulting in strong directional coupling. Typically for thicknesses less than  $30\mu\text{m}$  the mode spacing in the overlay is sufficiently large that variation of the  $V$  number from a matching condition leads to complete decoupling before coupling again to the next adjacent mode. Hence, as the overlay index or the input wavelength is varied, a periodic transmitted intensity response is observed (Figs. 2 & 3 respectively) as individual high order modes are tuned in and out of resonance with the fibre mode. The overlay may be passive in which case channel selection elements (wavelength division demultiplexers, WDMs) may be formed. Alternatively, the use of electro-optic, acousto-optic or semiconductor materials will lead to modulators, tunable WDMs or routing switches (if a second fibre block is used).

Based on the above basic device structure three practical methods of realising a frequency translator have been proposed and one method for an isolator. In the case of the former, attention was focused on methods involving the use of surface acoustic waves (SAWs) in a lithium niobate overlay to induce matching of the fibre and overlay mode propagation constants (ie effective indices). During fabrication, a slice



of lithium niobate is bonded to a polished fibre block, polished to a thickness of  $<30\mu\text{m}$  (see Fig.1 for basic structure) and tuned such that there is a particular mismatch in the effective indices of the fibre and the highest order overlay mode at the intended wavelength of operation. An interdigital electrode (IDE) structure fabricated on the top surface of the niobate by standard photolithographic techniques enables surface acoustic waves to be launched into the overlay, the acoustic frequency/wavelength having been selected to induce effective index matching (Fig.4). On excitation, it is proposed that optical power is coupled into the overlay and is shifted in frequency by an amount equal to the acoustic frequency. A second polished fibre block evanescently coupled to the top surface of the niobate and appropriately aligned may be used to collect the frequency shifted output. It is envisaged that such a structure will lead to excellent carrier suppression and efficient conversion. However, fabrication difficulties associated with the influence of the second fibre block on the matching condition and on the acoustic propagation are recognised.

In an alternative arrangement of the above device it has been proposed that the overlay is tuned to provide coupling in the absence of the acoustic wave. The operating characteristics of such a device on excitation of the acoustic wave are a little uncertain. However, issues which may be addressed include the loss of coupling, if any, due to the presence of the acoustic wave and the possibility of inducing coupling in the lithium niobate from the overlay mode matched to the fibre to an adjacent overlay mode. In the former case it is envisaged that frequency shifted light would appear in the transmission output fibre. The latter case is likely to yield a high conversion efficiency but will suffer from severe fabrication difficulties associated with matching of the acoustic wavelength to the beat length of the two adjacent overlay modes and the return of the frequency shifted and effective index shifted output to the original fibre or to a second fibre.

The second proposed approach is to tune the device for maximum coupling of power into the overlay in which interaction with a surface acoustic wave takes place in the Bragg regime. An interdigital electrode (IDE) pattern is used to generate the SAW which crosses the optical axis of the device at the Bragg angle (Fig.5). In such an arrangement the optical power coupled into the overlay is simultaneously deflected into the first order diffraction direction and frequency translated by an amount equal to the frequency of the SAW. The output is then collected by a second polished fibre block.

The final approach, based on the same basic device structure, involves the use of a SAW in a lithium niobate overlay to induce coupling between the  $LP_{11}$  and  $LP_{01}$  modes of an elliptical core fibre used in the formation of the polished fibre block. The overlay is tuned such that there is no optical coupling and the chosen device geometry simply enables good acoustic and optical contact between the overlay and the fibre.

The proposed optical isolator structure is shown in Figure 6. The interlay is formed of magneto-optic material bonded to the lower fibre block, polished to form a multimode planar waveguide of thickness less than  $30\mu\text{m}$  and tuned for maximum power coupling out of the fibre. The thin ( $<100\text{\AA}$ ) metal layer deposited onto the input fibre block constitutes a leaky mode surface plasmon polariser<sup>3</sup> and defines a linear TM input polarisation state. By application of an appropriate magnetic field to the interlay, Faraday rotation of the input polarisation by  $45^\circ$  may be achieved. Back reflected power from the output optical path will suffer a further  $45^\circ$  rotation and will be rejected by the thin metal film.

The aims of the programme are to develop at least one of the frequency translator options and the isolator. All of the proposed device configurations are based on the interaction between a high index multimode waveguide overlay and the side polished optical fibre to which it is evanescently coupled. In addition, most require the device output to be transferred to a second polished fibre block appropriately aligned on the top surface of the overlay (Fig.6). These requirements define the major features of the initial phase of the work programme as follows :

- Development of a comprehensive understanding of the coupling between a side polished single mode optical fibre and a high index, multimode planar waveguide overlay in evanescent contact with it (Fig.1).
- Definition of the design rules for wavelength selective fibre optic overlay devices
- Development of the fabrication techniques and skills for the realisation of polished solid state overlays such as lithium niobate
- Characterisation of the coupling to such overlays including an investigation of techniques for precisely tuning the position of the resonances ie tuning of the overlay mode effective indices relative to that of the fibre.

- Investigation of the coupling through the high index overlay to a second polished fibre addressing such issues as coupling efficiency, insertion loss, wavelength shifts etc.

and in parallel with the above

- A detailed device design exercise addressing such issues as the selection of the acoustic frequency, the electrode design etc for the frequency translator and the magnetic field magnitude and method of application for the isolator
- Realisation of device operation with the demonstration of frequency shifting and Faraday rotation in overlays of the respective devices without coupling to an output fibre.
- Demonstration of full device operation with fibre optic output.

## 2. PRELIMINARY INVESTIGATION OF FIBRE OPTIC OVERLAY DEVICES

### 2.1 Basic Theory

A great deal of insight into the operation of fibre optic overlay devices (Fig. 1) may be gained by assuming weak coupling with the response being determined by the dispersion of the planar multimode waveguide in contact with the fibre. The eigenvalue equation of the  $m$ th order mode of the overlay is :

$$\frac{2\pi d}{\lambda} (n_o^2 - n_{eo}^2)^{1/2} = m\pi + \varphi_1 + \varphi_2 \quad (1)$$

where  $\lambda$  is the input wavelength,  $d$  is the overlay thickness and  $\varphi_1$  and  $\varphi_2$  are the phase shifts associated with the boundaries of the overlay.  $\varphi_1$  and  $\varphi_2$  are given by:

$$\varphi_{1(i=1 \text{ or } 2)} = \tan^{-1} \zeta \left( \frac{n_{eo}^2 - n_i^2}{n_o^2 - n_{eo}^2} \right)^{1/2} \quad (2)$$

where  $\zeta = 1$  for TE modes and  $n_o^2/n_i^2$  for TM modes,  $n_i$  is the index of the fibre cladding and  $n_2$  is the index of the material in contact with the top surface of the overlay.

Efficient coupling of power from the fibre to the overlay is achieved when the effective index ( $n_{eo}$ ) of the highest order overlay mode, close to cut off, equals the fibre effective index,  $n_{ef} = 1.451$ , and the precise coupling condition may be obtained simply by substituting  $n_{eo} = n_{ef}$  into equations (1) and (2). For thick overlays the mode number  $m$  of the coupled mode is large and the terms  $\varphi_1$  and  $\varphi_2$  are small in comparison to  $m\pi$ . In addition, for symmetrically bound overlays,  $n_1 = n_2$  (eg if a second fibre block is used to collect the coupled power) and since  $n_{ef} \approx n_i$  with  $n_o \gg n_{ef}$  the inverse tan functions are small relative to  $m\pi$  even for thin overlays. Hence, for thick overlays supporting many modes or for symmetrically bound overlays  $\varphi_1$  and  $\varphi_2$  may be set to 0 in equation (1) and the coupling condition is approximated by :

$$2d(n_o^2 - n_{ef}^2)^{1/2} = m\lambda \quad (3)$$

Equation 3 gives the wavelength position of the resonances for any particular overlay refractive index and thickness. In general the overlay material choice (and hence the

material index) will be fixed by the device application. Hence, the overlay thickness,  $d$ , becomes the critical control parameter in determining the positions of the resonances and the resonance spacing.

## 2.2 Resonance Spacing ( $\Delta n$ )

In preliminary studies of device characteristics Cargille refractive index oils with known temperature coefficients of refractive index ( $\delta n/\delta T$ ) were used in the role of the overlay. The oil was introduced into a cavity defined by mica spacers between the polished fibre block and a quartz superstrate of index  $n_2 = 1.447$ . The device transmission characteristics as a function of temperature and hence refractive index (given  $\delta n/\delta T$ ) were then obtained (e.g. Fig.2 for a  $23\mu\text{m}$  oil overlay) for various oil indices and spacer thicknesses. From these response curves the material index shifts ( $\Delta n$ ) necessary to tune the matching condition from one mode to the next (ie the difference between the minima) were measured and plotted against index for each of the thicknesses  $30\mu\text{m}$  and  $60\mu\text{m}$  (Fig.7). Using equation 2 it is a simple exercise to calculate these index shifts. The calculated values are also plotted in Figure 7 showing good agreement with experiment. It should be noted that these device structures demonstrate good resonance depths in excess of 95% and low losses of  $<0.2\text{dB}$  off resonance (Fig 2 & 3).

## 2.3 Index and Wavelength Response

Variation of the input wavelength results in modulation of the mode effective indices of the overlay and leads to a periodic transmission function (Fig.3) as the individual high order modes are tuned in and out of resonance with the fibre mode. Hence, an alternative method of investigating the basic coupling characteristics of the device is to measure its transmission as a function of wavelength. Wavelength responses were, in fact, determined using a white light monochromator adapted for fibre use and, since waveguide and/or material birefringence may be present in the overlays used, a fibre polarisation controller was used in the input lead to define either a TE or TM mode at the device (Fig.8). Under typical measurement conditions the wavelength resolution was about  $2\text{nm}$  for a dynamic range of  $13\text{-}20\text{dB}$  depending on the launch conditions and system losses. Such a technique is more suited to all solid state devices in which the overlay material has a small  $\delta n/\delta T$ . To generate either a wavelength or index response in the region of a resonance it is essentially the effective index of the highest order mode which is being modulated relative to the fibre effective index. Depending on the application we may require a knowledge of the wavelength changes,  $\delta\lambda$ , the

material index changes,  $\delta n_o$  or the mode effective index changes,  $\delta n_{eo}$  across the width of a resonance (eg for the development of wavelength selective components, electro-optic modulators or acousto-optic devices respectively). It is therefore useful to derive relationships between these parameters so that, for instance, mode effective index or material index information may be derived from wavelength responses. In this context the following relationships have been derived by simple differentiation of equation (1) with  $\varphi_1$  and  $\varphi_2$  assumed to be negligible :

$$\delta n_{eo} = \delta n_o n_o / n_{eo} \quad (4)$$

and

$$\delta n_{eo} = -\delta \lambda (n_o^2 - n_{eo}^2) / \lambda n_{eo} \quad (5)$$

Dividing (4) by (5) yields an expression which relates a change in wavelength  $\delta \lambda$  to the change in material index,  $\delta n_o$ , which will induce an equivalent change in the mode index as follows :

$$\delta n_o = -\delta \lambda (n_o^2 - n_{eo}^2) / \lambda n_o \quad (6)$$

Figure 9 shows the thermally induced index response (a) and the wavelength response (b) in the region of a resonance for a device incorporating a  $23\mu\text{m}$  overlay of 1.504 index oil. From Fig 9b the full width half maximum (FWHM) linewidth,  $\delta \lambda$ , is  $28\text{nm}$ . According to equation (6) this linewidth is equivalent, in terms of mode effective index change, to a material index change of  $2.12 \times 10^{-3}$ . From Fig.9a the directly measured resonance width (FWHM) in terms of material index change, is  $2.02 \times 10^{-3}$ .

## 2.4 Resonance Linewidth ( $\delta \lambda$ )

Fibre optic overlay device structures are highly wavelength selective (Fig.10) and performance parameters such as the resonance linewidth ( $\delta \lambda$ , FWHM) are of particular importance in terms of the operation of specific devices like the frequency shifter or isolator. The wavelength sensitivity arises from the highly dispersive nature of the overlay mode effective indices ( $n_{eo}$ ) and the precise response around a resonance is determined, therefore, by the wavelength dependence of  $n_{eo}$ , for a particular overlay mode, relative to the fibre effective index. Hence, the linewidth will vary inversely with the rate of change of  $n_{eo}$  with  $\lambda$  ( $dn_{eo}/d\lambda$ ) for the particular mode on resonance. The parameter,  $dn_{eo}/d\lambda$ , is strongly dependent on the overlay index ( $n_o$ ) and thickness and it may be evaluated numerically using equation (1) as a function of these variables. Figure 11 shows a plot of  $(dn_{eo}/d\lambda)^{-1}$  versus index for two overlay thicknesses,  $d$ , of  $12\mu\text{m}$  and  $23\mu\text{m}$  using an input wavelength of  $1300\text{nm}$ .

It is anticipated that the linewidth will follow the trend defined by  $(dn_{eo}/d\lambda)^{-1}$  and will increase with decreasing  $n_o$ , with particularly rapid increase below  $n_o = 1.55$ . Fig 12 shows the variation of  $(dn_{eo}/d\lambda)^{-1}$  with thickness,  $d$ , at  $\lambda=1300\text{nm}$  for  $n_o = 2.2$  (corresponding to lithium niobate). This indicates that the linewidth should increase with decreasing thickness with particularly rapid increases at thicknesses less than  $10\mu\text{m}$ .

From coupled mode theory<sup>4</sup> it is expected that the linewidth will decrease with decreasing coupling strength between the fibre and the overlay i.e. with increasing remaining cladding thickness on the polished fibre. To test this and the other trends with  $n_o$  and  $d$  discussed above, three polished fibre blocks were fabricated with different remaining cladding thickness such that the coupling of power from the exposed core fibre into bulk material of index 1.6 was 24%, 50% and 98%. The wavelength response (example in Fig.10) and the resonance linewidth were then measured as a function of overlay index for each block at two thicknesses,  $d$ , of  $12\mu\text{m}$  and  $13\mu\text{m}$ . In each case the resonance closest to  $1300\text{nm}$  was used for the linewidth measurement. Figures 13 and 14 present the results for the  $12\mu\text{m}$  and  $23\mu\text{m}$  overlay thicknesses respectively. Clearly the linewidth increases with decreasing overlay index  $n_o$  and closely follows the trend of increasing  $(dn_{eo}/d\lambda)^{-1}$  with  $n_o$ . In addition narrower linewidths were observed with increasing thickness and decreasing coupling strength as predicted above.

## 2.5 Conclusion

In conclusion the preliminary investigations using oils have been useful in consolidating our basic concepts of fibre optic overlay device operation and in providing an appreciation of device characteristics in terms of modulation depths, losses, resonance widths, wavelength response, index response etc. In addition the experimental results have been used to validate a number of simple equations which will be useful in the interpretation of future studies on solid state overlay devices.

### 3. ALL SOLID STATE FIBRE OPTIC OVERLAY DEVICES

#### 3.1 Device Fabrication

The simplest technique for the fabrication of solid state overlay devices is by the vacuum deposition of dielectric thin films directly onto a polished fibre block. Such a technique generally is only useful for the realisation of passive structures such as fixed wavelength WDMs. Active devices require the use of crystalline materials such as lithium niobate which offers piezoelectric, electro-optic or acousto-optic properties. Such materials may be used in the realisation of fibre optic overlay devices by bonding a thin slice of material to the polished fibre block and polishing it to a thickness in the region of 5-30 $\mu$ m. A large proportion of the programme effort was spent on this area with the result that most of the problems have been identified and solved. The major issues influencing the successful realisation of a device include the topology of the polished fibre block, the bonding of the overlay to it and the maintenance of the overlay parallelism and integrity during the polishing process. The optical fibre is embedded in a groove cut in a quartz block and fixed using an epoxy. If either the fibre or the epoxy is not perfectly flush with the surface of the polished quartz, proud being the worst case, then the overlay material becomes stressed in this region leading to break up (Fig. 15a) or poor surface topology during polishing (Fig. 15b). It may also lead to wedged bonding and a wedged overlay which results in broad shallow resonances ie a poor response function. The solution to this problem lies in the selection of the epoxy, the allowance of a stabilising period before polishing (during which the epoxy may shrink or swell) and the absence of any solvents from the cleaning processes (solvents cause the epoxies to swell). Even after adoption of such measures, there is only a small yield of suitable blocks which are selected via a screening process.

The main issues associated with the bonding of the overlay to the fibre block are the achievement of bond parallelism and strength. Non-parallelism leads to wedged overlays resulting in poor response functions and lack of strength leads to overlay break up (Fig. 15a) or even complete loss. Again the critical issue in terms of success is the selection of the bonding media. Unfortunately the solution to both problems places conflicting requirements on the choice. To ensure high parallelism it is better to use adhesives of very low viscosity such as a UV curing agent and thereby obtain a very thin parallel bond. Such adhesives, however, lack the strength of epoxies which are highly viscous and lead to thick bonds with the associated difficulties of obtaining good parallelism. Many epoxies and UV curing adhesives have been used and the



greatest success has resulted from epotek 301 and Luxtrak UV adhesive by ICI. An alternative approach to mounting the overlay which has yielded some success is to polish it to around  $100\mu\text{m}$  while it is mounted by wax to a flat ( $<\lambda/4$ ) glass support disc. On de-mounting it is very flexible and it may be "rung" to a flat ( $<\lambda/4$ ) polished fibre block. Adhesive is then used to bond down the edges before subsequent polishing to sub  $30\mu\text{m}$ .

The degree of overlay parallelism determines the quality of the device response in terms of resonance sharpness (width) and depth. Typically for the oil results presented previously the resonance width (FWHM) in terms of mode effective index was  $\delta n_{\text{eo}} = 0.001$ . Differentiating equation 1 with respect to thickness yields :

$$\delta n_{\text{eo}} = \delta d(n_o^2 - n_{\text{eo}}^2) / n_{\text{eo}} d \quad (7)$$

Letting  $n_{\text{eo}} = n_{\text{ef}} = 1.451$ , the thickness change,  $\delta d$ , to induce an effective index change,  $\delta n_{\text{eo}} \sim 0.001$ , in a  $20\mu\text{m}$  lithium niobate overlay ( $n_o = 2.2$ ) is  $11\text{nm}$ . This means that to obtain a resonance with  $\delta n_{\text{eo}} = 0.001$  in such an overlay device requires that the deviation from parallelism is less than  $11\text{nm}$  over the  $1\text{mm}$  interaction length of the device. The necessary angular control to achieve this during polishing is 2 arc second and the situation deteriorates with decreasing overlay thickness. Logitech provide precision polishing jigs and recommend sophisticated procedures for the achievement of precise angular control and parallelism. However, the required results are on the very edge of this capability.

The accumulated difficulties noted above resulted in a yield problem and, often, many painstaking weeks of work were required to produce one useful device. Thereafter, for the frequency translator, precise resonance tuning is required followed by the production of interdigital electrodes by vacuum deposition and photolithographic processes leading to an ever increasing probability of device failure. Herein lies the rate determining step in the project and yield remained a problem till the end.

### 3.2 Zinc Sulphide, Zinc Selenide and Glass Overlay Devices

In an effort to gain some preliminary experience of the characteristics and fabrication of solid state overlay devices before using lithium niobate or BIG, several structures were fabricated by vacuum deposition of ZnS or ZnSe and by processing BK7 glass using the bonding and polishing techniques described above. The wavelength characteristics were measured using a white light source and a monochromator

adapted for fibre use and, since either waveguide and/or material birefringence may be present, a polarisation controller was used in the input lead to establish either a TE or a TM mode at the device (Fig.8). Under typical measurement conditions the wavelength resolution is in the 1-2nm region for a dynamic range of 13-20dB. Figures 16 and 17 show the wavelength responses of a 2.5 $\mu$ m thick ZnS overlay device and a 17 $\mu$ m BK7 structure. The devices were not capped and, hence the superstrate index  $n_2$  was 1. As expected, strong polarisation sensitivity is observed and the response shown is for the TM polarisation. By application of a capping layer matched to the cladding index (ie  $n_2 = n_1$ ) the resonances, although now shifted in position, did not exhibit any detectable polarisation sensitivity. Overall this work demonstrated that good modulation depths (>95%), low loss (<0.2dB) and relatively sharp resonances (20nm and 8nm for the glass and ZnS respectively) may be obtained using the proposed fabrication techniques.

Once an overlay device has been fabricated, it is necessary to finely tune its resonance position to match the source wavelength i.e. the wavelength of operation. Inspection of the waveguide equation (1) indicates that this may be achieved by variation of the refractive index of the superstrate material,  $n_2$ , which interacts with the evanescent field of the coupled overlay mode. Simply applying bulk material of appropriate index to the top surface of the overlay will therefore achieve the desired result. Alternatively, the effective index of the superstrate may be varied by the vacuum deposition of a low index film where the film thickness is controlled to select the resonance position.

To investigate the influence of superstrate index Cargille refractive index oils were used in the role of the superstrate with a BK7 polished glass and a vacuum deposited ZnSe overlay. Figure 18 shows the TE mode wavelength responses of a 7.25 $\mu$ m thick BK7 overlay device ( $n_0 = 1.504$ ) for superstrate indices  $n_1 = 1$  (air), 1.452, 1.454 and 1.456 (Cargille oils). The theoretical (solid line) and experimental variations of the TE and TM resonance position with superstrate index (in the range 1.39-1.45) are then plotted in Figure 19. Figure 20 presents the TE wavelength response of a 1.5 $\mu$ m thick ZnSe device ( $n_0 = 2.47$ ) with an air superstrate and the theoretical (solid lines) and experimental variation of the resonance position with superstrate index is presented in Figure 21. Clearly the resonance position may be tuned by several 10s of nanometers after production of an overlay device by variation of the superstrate index and the index required may be accurately predicted from equation (1).

To assess the feasibility of tuning by thin film deposition the resonance position of the  $7.25\mu\text{m}$  BK7 device was measured as a function of the thickness of a magnesium fluoride layer ( $n_2 = 1.38$ ). The tuning curves for the TE and TM resonance positions are given in Figure 22. Again, it is clear that this method may be used to finely tune the resonance position by a few 10s of nanometers. This technique would probably be adopted in practice with on-line monitoring of the resonance position during vacuum deposition.

### 3.3 Lithium Niobate Overlay Devices

Several 'good quality' lithium niobate overlay devices have been produced by the polishing techniques described above (the criteria for "good quality" being highly parallel, unbroken overlays yielding useful response functions). Figures 23 and 24 show the TM and TE wavelength response curves for a  $20\mu\text{m}$  lithium niobate overlay device. Resonance widths are in the region of 2-4nm and >95% of the launched power coupled to the overlay on resonance. Losses, off resonance are again <0.2dB. Such characteristics in the basic fibre overlay device are ideal for further processing to yield a frequency translator.

To yield frequency translators the fibre optic overlay device must be tuned either on resonance at the operational wavelength or off resonance by a fixed predetermined amount. One way to tune the system is by further precision polishing which is stopped at the precise required thickness. On resonance devices have been realised in this manner. An alternative is to produce the overlay device at approximately the correct thickness, measure its wavelength response and then tune the resonance position by applying a capping layer (superstrate). The superstrate may be a bulk material of the required refractive index or it may be a vacuum deposited film of fixed material index ( $<n_{ef}$ ) in which case the film thickness acts as the tuning control parameter. To assess the potential resonance tunability, the TE and TM wavelength responses of a  $10\mu\text{m}$  thick overlay device were measured with various bulk oil superstrates in the index range 1.40 to 1.45. In Figure 25, the measured shift in resonance position,  $\Delta\lambda$ , relative to that for a superstrate index of 1 (ie air) is plotted against superstrate index for both TE and TM modes. The theoretical relationships obtained using equation 1 are also presented. Clearly from Figure 25 there is a potential tuning range of up to 20nm. One proposed tuning technique which offers some practical merits is the vacuum deposition of Calcium Fluoride ( $n=1.40$ ) controlling its thickness as the tuning parameter. From Figure 25, a bulk superstrate of index 1.40 shifts the resonance position relative to that for air by 12nm (TM

polarisation). This implies that a 12nm tunability may be obtained using the calcium fluoride technique. This technique will probably be adopted in practice with on-line monitoring of the resonance position during vacuum deposition. Fig.26 shows the theoretical variation of the TM resonance position for a 10 $\mu$ m thick lithium niobate overlay as a function of CaF<sub>2</sub> thickness (obtained by the Matrix Method)

In most of the proposed designs of frequency translator and in the optical isolator a second polished fibre block is required to collect the output. Figures 26 and 27 show the TE and TM wavelength responses respectively of both the transmitted and coupled arms of a 10 $\mu$ m lithium niobate overlay device coupled to a second polished fibre. These results demonstrate that up to 90% of the launched power may be coupled from the input fibre through a multimode waveguide interlay into a second aligned fibre. It is believed, therefore, that the insertion loss of the proposed devices may be reduced to acceptable levels in the 1-3dB region. On application of the second polished fibre block it was noted that the resonance position for the TM and TE modes respectively shifted by 20.2nm  $\pm$  0.5nm and 7.5nm  $\pm$  0.5nm. These shifts must be accommodated in the tuning of the fibre optic overlay device.

### 3.4 Magneto-optic Overlay Devices

The fabrication of magneto-optic overlay devices presents several interesting practical problems which are not insurmountable but are probably best described as daunting. BIG, the only material with a sufficiently high Verdet constant, is only available in 2mm square by 300 $\mu$ m thick layers epitaxially grown on GSGG at a cost of approximately \$1000. Furthermore the plane of the slice is perpendicular to the most efficient magneto-optic axis. Using the material in the plane of the supplied slices approximately halves the magneto-optic efficiency which does not preclude the realisation of usable devices. The primary problems lie in the handling, bonding and polishing of such a small sample of the wrong orientation.

Attempts were made to fabricate overlay structures using the bonding and polishing techniques described above. However, the handling problems precluded the realisation of any useful devices. Eventually, it was decided to terminate work on this approach to optical isolation by mutual agreement with project monitor (see quarterly report May 1992).

#### 4. ACOUSTO-OPTIC FREQUENCY SHIFTER: DESIGN CONSIDERATIONS

It has long been understood that an acoustic wave travelling through a material causes the refractive index of the material to be modulated in a periodic manner where the periodicity is defined by the frequency of the acoustic wave. Furthermore, light can be made to interact with a moving grating of this type such that some, or all, of the light is scattered and doppler shifted in frequency by an amount proportional to the periodicity of the grating<sup>5-7</sup>. Much research has been carried out with the aim of harnessing this phenomenon to produce frequency shifting components suitable for use in optical sensing and communications applications<sup>8-9</sup>. The bulk of the research effort, however, has concentrated on the development of planar waveguide or integrated optical technologies. Such device geometries are not readily compatible with optical fibre systems. The aim of this current work is to address the problem of manufacture of a frequency shifting component constructed around an uninterrupted length of fibre. The three main techniques proposed above are now considered here in terms of the acoustic design.

##### 4.1 Evanescently Coupled Bragg Frequency Shifter

Using the mechanism of evanescent coupling, power may be transferred between an optical fibre and a waveguide in close proximity. If the waveguide is made of an active material the light may be modulated in some manner (eg frequency or phase) and then recoupled back to the original guiding fibre or alternatively to an additional fibre positioned above the overlay layer. In the device proposed here light coupled into the overlay interacts with a SAW at the Bragg angle,  $\alpha_b$  and is diffracted (Fig.5). The first order diffracted beam is frequency shifted by the SAW frequency and may be collected by a second polished fibre block.

The process of acousto-optic interaction is depicted in Figure 29. An acoustic wave is made to traverse the path of an optical beam. In general such a wave will cause the light to be diffracted into a number of discrete beams. If however the acoustic beam and the optical beam intersect at the appropriate angle ( $\alpha_b$  the Bragg angle), then reflections from successive wave fronts add in phase and a single diffracted order is produced. Under such conditions the angular relation between the incident and diffracted beam is described by :

$$\sin \alpha_b = \lambda / 2n\lambda_a \quad (8)$$

where  $\lambda$  is the optical wavelength and  $\lambda_a$  is the acoustic wavelength. An efficient interaction between the optical wave and the acoustic wave is achieved when the optical beam width is such that it is traversed by a number of acoustic wavelengths. In general the efficiency of the diffraction process can be quantified by the device quality factor  $Q$ ,

$$Q = 2\pi\lambda L / n\lambda_a^2 \quad (9)$$

where  $L$  is the effective acousto-optic interaction length. From Klein and Cook<sup>10</sup>, an approximate lower value of  $Q = 4\pi$  defines the criteria for efficient Bragg operation. In the arrangement considered here, the geometry of the launch and capture fibres imposes limitations which are not generally encountered in the design of acousto-optic devices. The width of the optical beam must be restricted in order that efficient transfer of the energy to the capture fibre can be achieved. In order that the optical path be exposed to a sufficiently large number of grating periods, the frequency of the acoustic wave must be such that the acoustic wavelength is smaller than the fibre core dimensions. Table 1 illustrates the effect of operating frequency on the acoustic wavelength and the required acousto-optic interaction length for efficient operation. Inspection of this table reveals that at an operating frequency of 500MHz the acoustic wavelength approaches the dimensions of the fibre core. Furthermore, an interaction distance of 168 $\mu$ m is required to achieve efficient acousto optical coupling. This distance is comparable with the interaction length required to couple optical energy from one fibre to another using this geometry. Therefore at this frequency efficient Bragg scattering and capture of the diffracted beam becomes possible.

The design of interdigital transducers, IDT, to produce a high frequency Surface Acoustic Wave (SAW) is a complicated procedure and requires consideration of both the mechanical and electrical characteristics of the medium. Fortunately a considerable amount of attention has been given to this problem by radio engineers concerned with the problem of constructing analogue delay lines at microwave frequencies. A simplified model has been developed by Smith et.al<sup>11,12</sup> which allows the mechanical impedance of the piezo- electric substrate to be related to the electrical impedance of the driving source. It is thus possible to attain conditions where both are matched and efficient electro-acoustic conversion can be achieved. The electrical resistance,  $R_o$  of the IDT under resonant conditions can be described by :

$$R_o = 2\pi / (\omega_o C_s k^2) \quad (10)$$

where  $\omega_0$  is the angular frequency of operation,  $C_s$  the transducer capacitance per section and  $k$  the effective electro mechanical coupling efficiency of the material. The overall bandwidth of the energy transfer is determined by the smaller of the acoustic and electrical bandwidths. Increasing the number of transducer sections increases the efficiency of acoustic wave generation. However this also decreases the acoustic bandwidth. Under resonant conditions, an optimum number of transducers pairs,  $N$ , is found to exist depending only upon the electro-mechanical coupling constant  $k$ :

$$N^2 \sim \pi / 4k^2 \quad (11)$$

The acoustic aperture is determined by the length of the transducer finger, which in turn can be related to the impedance of the transducer and matched to the electrical drive circuitry. Thus the acoustic aperture ( $L$ ) is limited by:

$$C_s = 2\pi C_{ff} v_s L / \omega_0 \quad (12)$$

where  $C_{ff}$  is the capacitance of individual fingers and  $v_s$  is the sound velocity equation. The design features of a 500 MHz transducers are listed in Table 1 for the particular case of X-cut  $\text{LiNbO}_3$ . It is interesting to note that for all frequencies of operation with this particular orientation of  $\text{LiNbO}_3$  the optimum transducer length is  $112\lambda_a$ .

#### 4.2 Acousto Optic Frequency Shifter: Modulation of coupling to the Overlay

Optical power couples efficiently between two co-linear waveguides in close proximity provided that the propagating modes in each guide are matched in effective index ( $n_e$ )/propagation constant ( $\beta$ ). Where the two guides have different propagation constants coupling may be achieved by the application of a periodic perturbation (e.g. a periodic refractive index variation in one of the guides) such that the perturbation period equals the beat length ( $L_B$ ) between the guides. This is the basis of the grating assisted coupler<sup>13,14</sup>. Furthermore, if the periodic perturbation is moving, as in the case of a surface acoustic wave (SAW), the coupled power will be frequency shifted<sup>15</sup>.

In fibre optic overlay structures the effective indices (i.e. propagation constants,  $\beta$ ) of the overlay modes are highly wavelength dependent. Hence, the wavelength response is periodic as individual modes are tuned in and out of resonance (i.e. propagation constant matching) with the fibre mode. Application of a SAW to the overlay, therefore, will induce coupling at wavelengths for which there is a given mismatch

( $\Delta\beta$ ) in propagation constant between the fibre mode and the overlay modes. Coupling will then occur at the wavelengths for which the beat length ( $L_B$ ) between the fibre and the overlay modes is equal to the SAW period.

At any particular wavelength the mismatch in propagation constant,  $\Delta\beta$ , between any given overlay mode and the fibre mode may be related to the beat length  $L_B$  by

$$\Delta B = 2\pi / L_B \quad (13)$$

and the corresponding mismatch in effective index  $\Delta n_{eo}$  may be found from

$$\Delta B = 2\pi\Delta n_{eo} / \lambda \quad (14)$$

By simple differentiation of equation (3) the change in wavelength,  $\Delta\lambda$ , which results in a mode effective index change of  $\Delta n_e$  in the overlay is given by

$$\Delta\lambda = \frac{\lambda n_{eo} \Delta n_{eo}}{n_o^2 - n_{eo}^2} \quad (15)$$

Application of a surface acoustic wave to the overlay will result in coupling at new wavelengths somewhere between the steady state resonant wavelengths and new resonances will appear in the wavelength response of the device. Given that to achieve coupling the SAW period must be equal to the beat length,  $L_B$ , between the two modes mismatched in effective index by  $\Delta n_{eo}$ , the above equations may be used to calculate the shift in the wavelength position of the resonance,  $\Delta\lambda$ , due to interaction with the SAW, for any given SAW period. The design criterion adopted here is that we should seek to induce SAW resonances precisely midway between two steady state resonances. From (3) it is a simple matter to show that the change in effective index  $\delta n_{eo}$  between two adjacent overlay modes is given by

$$\delta n_{eo} = \lambda(n_o^2 - n_{eo}^2)^{1/2} / 2dn_{eo} \quad (16)$$

and  $\Delta n_{eo}$ , for the purpose of designing the SAW device, therefore, should be equal to  $\delta n_{eo}/2$  to meet the above criterion. The parameter,  $\delta n_{eo}$ , is dependent on the overlay thickness, and hence the choice of SAW period (and frequency= period x velocity, 3488m/s is lithium niobate) to meet the design criterion is also thickness dependent. The SAW drive frequency,  $\delta n_{eo}/2$  and  $\Delta\beta$  calculated for various values of  $d$  using the



above relationship are presented in Table 2. The interdigital electrode spacing to generate the SAW is simply equal to the SAW period. In the fabrication of devices reported here the target overlay thickness was  $25\mu\text{m}$  implying an ideal SAW period of  $87.8\mu\text{m}$  corresponding to a drive frequency of  $39.7\text{MHz}$ . In practice the SAW period was  $80\mu\text{m}$  ( $f = 43.2\text{MHz}$ ).

It had also been proposed that the application of the SAW wave would result in loss of the steady state coupling and that power remaining in the fibre at the steady state resonant wavelengths would be frequency shifted. This could also be assessed in the same device structure.

### 4.3 Fibre Mode Coupled Frequency Shifter

In addition to the two areas outlined above, a third approach to the design of a frequency shifting device under investigation involves coupling from the  $\text{LP}_{11}$  mode of an optical fibre to the  $\text{LP}_{01}$  mode. Devices of this nature have been investigated by a number of laboratories<sup>16-19</sup>, the most common approach being to introduce a travelling acoustic wave along a fibre length with the use of an acoustic horn. Additionally, an arrangement whereby an optical fibre was brought into intimate contact with a SAW on a PZT substrate has also been investigated. The current approach will use a technique similar to the latter approach, however it is intended that an elliptical core fibre be polished such that the core comes into close proximity with the acoustic energy. In this manner it is intended to increase the overall efficiency of the device. The beat length of the elliptical core fibre has been measured to be  $75\mu\text{m}$  thus interaction over approximately 30 cycles would be possible over a length of  $2\text{mm}$ .

## 5. OPTICAL ISOLATOR DESIGN

The development of coherent communication and optical fibre sensing systems has stimulated a requirement for the development of low loss components which provide high degrees of optical isolation. It is intended that the techniques developed during the investigation of the evanescently coupled fibre optic components be applied to this area. The proposed device geometry is as indicated in Figure.6

A standard means of achieving optical isolation is through the use of a magneto-optic crystal and a polarisation selective element. Under the influence of an applied magnetic field the magneto-optic crystal produces a rotation in the polarisation state of the optical field travelling through the crystal. The length over which this interaction takes place and the strength of the magnetic field are both tuned such that a  $45^\circ$  rotation in polarisation is achieved. Light reflected back through the crystal is rotated by a similar amount and therefore emerges at the original input port orthogonal to the launch polarisation state. This light can therefore be readily attenuated with the use of a polaroid analyser at the system input. Typically devices of this type are constructed using such materials as Yttrium Iron Garnet (YIG) and Bismuth Iron Garnet (BIG). In order that it may be established whether or not the evanescently coupled construction would be suitable for an optical isolator of this design principle, the properties of the commonly used crystals had to be established.

The degree of polarisation rotation achieved under the Faraday effect can be tuned through control of the interaction distance and the strength of the magnetic field. For the YIG crystal, the required propagation distance is found to be approximately 3mm. This distance represents what might reasonably be termed the maximum interaction length of the polished block coupler. Construction of a device with a YIG active layer would therefore increase the already substantial problems associated with coupling to a high index active superstrate layer. BIG was therefore investigated as an alternative material, it is specified as having a required magneto-optic interaction length of approximately  $300\mu\text{m}$  under saturated field conditions. A sample of BIG  $2\text{mm} \times 2\text{mm} \times 400\mu\text{m}$  has therefore been purchased for experimental evaluation. In the material, as supplied, the most efficient magneto-optic interaction is obtained by propagation perpendicular to the plane of the slice. The proposed device geometry requires that propagation will lie in the plane of the slice in which case the magneto-optic efficiency is unknown, although, it is proposed to be about half that of the optimum geometry.

Attempts were made to fabricate a device using the BIG material. However, severe handling problems (see section 3.4) precluded the achievement of any useful overlay structure. In view of this, work on the isolator was terminated by agreement with the project monitor.

## **6. FABRICATION OF THE FREQUENCY TRANSLATOR**

Fabrication of devices can be divided broadly into three sections :

- (1) Production of side polished fibre blocks
- (2) Fabrication of multimode overlay waveguides
- (3) Fabrication of the interdigital electrode structure

### **6.1 Production Of Side Polished Fibre Blocks**

This follows the methods which have become well established in the production of tunable directional couplers.

A silica glass block of suitable dimensions ( $\sim 30 \times 15 \times 8\text{mm}$ ) has a groove cut in it which has an arc shaped depth profile along the length of the block. The diameter of the arc is in the range 250-300mm whilst its width is 0.13mm. The groove is designed to take a bare optical fibre of diameter 0.125mm with 0.005mm being allowed for the glue line. As will be described later it was found necessary to minimise the glue line width in order to successfully produce thin overlay waveguides. The ends of the grooves are sometimes opened out to a greater width in order to accommodate the fibre cladding and give the device greater strength. A piece of fibre, a suitable length of which has been stripped of its primary buffer using dichlormethane, is then bonded into the slot by the use of an epoxy resin. The fibre is held in the arc shaped groove by a jig consisting of clamps and small weights whilst the resin is cured by means of a heat gun.

After the fibre has been bonded into the silica glass block, the block is then waxed onto the pad of a polishing jig. Lapping and polishing are then used to remove some of the glass block and the fibre cladding until a point is reached where the evanescent field of the fibre is accessed. Lapping is carried out using first  $9\mu\text{m}$ , then  $3\mu\text{m}$ , alumina powder slurry on a glass lapping plate. This is followed by polishing with cerium oxide slurry on an expanded polyurethane plate. The degree to which the evanescent field is accessed is determined by measuring the difference in light transmission before and after a drop of high index oil is put onto the polished fibre surface. The fraction of light coupled out of the fibre will depend on how close the fibre has been polished to its core and this will be shown by a drop in throughput intensity. This method gives a relative rather than an absolute measurement of

evanescent field strength but it has been found to be extremely useful in establishing the characteristics necessary for device production. Since the fibre is in an arc shaped groove, the distance between the polished surface and the fibre core will be continuously varying, and hence the measured value will be related to the integral evanescent field over the effective interaction length.

## 6.2 Fabrication of the Multimode Overlay Waveguide

When the production of the side polished fibre block is complete, the plane of its polished surface will be parallel to that of the jig drive ring. The lithium niobate which is to form the multimode overlay must be bonded onto the block whilst it is still in situ in order to retain this parallelism. Since the niobate at this stage is 0.5-1.0mm thick it will be necessary to lap and polish it down to its required final thickness. It is crucial that the overlay has a high degree of parallelism between its bottom and top surfaces if sharp resonances are to be obtained. If the overlay waveguide is not parallel, then the propagation constant of its modes will vary along its length and hence the coupling conditions will be continuously changing. This will result in broadening of the resonances. The parallelism necessary to realise the sharpest resonances attained was about 2 second of arc (see Section 3.1).

Bonding the niobate to the fibre block was found to be one of the most crucial parts of the fabrication procedure. It is necessary that the bond line be thin and parallel and able to withstand all the subsequent processing. If the bond line is not parallel then it follows that the waveguide will not be parallel since the niobate will be polished parallel to the block surface. The subsequent processing stages (e.g. lapping, polishing, photolithography and aluminium etching) require that the bond line must have good shear strength and be able to withstand water, alkali, acid and certain solvents. The refractive index of the bond line is also important. If it is greater than the effective index of the fibre it will form part of the overlay waveguide with the niobate, but if it is less than, or equal to, the cladding of the fibre then it will form a buffer layer between the fibre and the niobate waveguide. In either case the refractive index and thickness of the bond line will have a significant effect on the coupling between the fibre and the niobate and hence on the depth and broadness of the transmission resonances. It is also necessary that the bonding material is optically transparent at the wavelength of device operation. In addition to considering the optical properties of the bond line, its acoustic properties must also be considered. The degree of penetration of the SAW into the bond line from the niobate will be dependent on the relative dimensions of the thickness of the niobate and the

wavelength of the SAW. The longer the acoustic wavelength, the greater will be its penetration depth. If the bond material has a propagation constant which is significantly different to that of niobate, or the bond layer is acoustically lossy, then the acoustic wave may be seriously attenuated as it propagates across the interaction region. The interaction region is of the order of 2-3mm long and the transducer will be positioned a short distance from it. It is difficult to quantitatively predict the acoustic behaviour of such a system theoretically, especially as the relevant acoustic parameters for epoxies are rarely available. Since, however, the niobate, the fibre and also the silica glass backing block will have similar acoustic properties, it is the behaviour of the bond line which will prove to be crucial.

To summarise, the bond layer between the niobate and the fibre block needs to have the following properties :

- it must be thin and parallel, therefore it must have a low viscosity when applied
- it needs to have good shear strength and chemical resistance to survive the polishing and electrode fabrication stages
- the optical properties need to be such that efficient, non lossy coupling is permitted between the fibre and the overlay to produce deep, sharp resonance points
- the bond layer must produce the minimum attenuation of the acoustic wave.

Because the properties of the bond line are so critical to the operation of a device, the investigation of this area took up a considerable amount of time. Many methods of bonding were considered but four principal methods were investigated in detail, these being :

- (a) Ringing the niobate onto the backing block (i.e. no bond layer)
- (b) Use of a very low viscosity light cured epoxy having a refractive index of 1.452 (= to cladding of fibre)
- (c) Use of a two part, room temperature curing epoxy having a refractive index of 1.52 (greater than the fibre effective index)

- (d) Use of phenyl salicylate, a compound which melts at 42°C to become a very low viscosity liquid. Its acoustic properties are compatible with those of glass.

**(a) Ringing of lithium niobate onto the fibre block**

Since this method avoids putting any bonding material between the fibre block and the lithium niobate this would be the ideal method if it proved practically possible. The method involves getting the surfaces of both the fibre block and the lithium niobate optically flat and then bringing them in contact by pressing them together. It is crucial also that both surfaces be absolutely clean as any contamination would prevent intimate contact.

It was found to be possible to ring the niobate on to the fibre block over a large enough area to produce a viable device. Since ringing did not extend over the full area, due mainly to edge rounding of the niobate, it was necessary to protect the edges with a wedge of epoxy before polishing could comment. Although, in several of the devices which were produced the bond survived the lapping process, it tended to deteriorate during further processing (to be described in section 6.3). This was because ringing did not occur where there was a glue line between the fibre and the glass block into which it was mounted. The most vulnerable area was at the end of the ellipse where the glue line is widest. To overcome this problem the fibre block fabrication process was modified to include the insertion of thin slivers of glass into the slot at either end of the groove and hence reduce the glue line. This was found, however, to be extremely intricate and time consuming and did not overcome the problem completely. It was reluctantly concluded that ringing the niobate on to the fibre block was not a viable alternative unless a method could be devised of making a glue-less fibre block. This would necessitate using a glass rather than an epoxy to bond the fibre into the block and it was not apparent how this might be achieved.

**(b) Use of low viscosity, low index light cured resin**

The light cured resin LCR 0001.46 (made by ICI) was the one most commonly used during the experiments. It has an extremely low viscosity (<1 poise) and a refractive index equivalent to that of silica. Unfortunately its adhesion is not as good as other higher index resins and neither is its chemical resistance. However, it was employed because it is, so far as we have been able to determine, the only available adhesive

which has such a low viscosity and refractive index. In order to protect the glue line during processing a wedge of tougher, more chemically resistive epoxy such as Epotek 301 was put round the niobate before lapping commenced. Wedging or other distortion of the niobate could be detected by observing the fringes produced by illumination from a helium single wavelength source bulb. This was done after the niobate had been lapped and polished down to its required thickness.

**(c) Use of room temperature curing 2 part epoxy**

Epotek 301 was tried since it combines good adhesion and shear strength with good optical transparency. Its refractive index is 1.54 which is greater than that of the fibre whilst its viscosity is  $>1$  poise. This makes it more difficult to obtain as thin and as uniformly thick a bond line as can be achieved when LCR 0001.46 is used. Also bubbles produced during the mixing of the 2 part resin were difficult to remove and tended to get trapped between the niobate and the fibre block. For these reasons it was decided not to proceed with this resin.

**(d) Phenyl Salicylate**

Phenyl salicylate is used as a bonding material where good acoustic transmission is required and thus it was suggested to us by Marshall Saylers that we try it for our application. It is solid at room temperature but melts at  $42^{\circ}\text{C}$  to form a very low viscosity liquid, thus offering the possibility of a very thin bond line. Since it is necessary that the fibre block remains on the polishing jig in order to accurately retain parallelism, the bonding process was awkward, since we felt it necessary to cool the assembly slowly to avoid producing strain. To overcome this the fibre block was warmed using a hot air gun whilst it was still on the jig and a small amount of phenyl salicylate was melted on its surface. The niobate was then pressed on to its surface and warmed to ensure that the salicylate remained fluid whilst a thin uniform bond line was obtained. To ensure slow cooling the jig was then inverted onto a prewarmed cast iron flat plate with a paper spacer to prevent sticking and left overnight to cool. In the morning it was found, however, that the salicylate had not solidified even though the temperature of the whole assembly was at least  $20^{\circ}$  below its melting point. Water had to be sprayed on to the sample to make it crystallise out. The edges of the niobate were protected with a wedge of tougher epoxy before lapping and polishing were attempted. The niobate was lapped down to approximately  $50\mu\text{m}$  before it became detached from the fibre block. In order to investigate further the properties of the salicylate a small quantity was melted in a beaker and allowed to



cool. It was again observed that cooling down to room temperature failed to cause it to solidify until nucleation was initiated by touching the liquid surface. When it did solidify it did so very rapidly leaving a structure of crystallites having a considerable amount of porosity. It was estimated that a shrinkage of ~20% took place upon solidification.

It was concluded that phenyl salicylate was not a suitable bonding material since it did not provide sufficient adhesion to withstand the lapping process. This could be due to (a) poor adhesion between the salicylate and the niobate or glass (b) inadequate sheer strength of the salicylate or (c) the stresses and porosity produced in the salicylate layer due to shrinkage upon solidification.

In view of the above the ICI Luxtrak LCR resin and process (b) became the favoured overlay bonding option. This approach was used exclusively in all further device fabrication.

Lapping and polishing of the niobate are carried out using processes similar to that for the fibre block. The main difference is that for polishing lithium niobate syton (a colloidal suspension of silica in an alkali solution) is used as the polishing medium rather than cerium oxide slurry. It was found by observing interference fringes that distortion of the niobate tended to take place in the region of the fibre glue line. The reason for this is that epoxy and silica glass polish at different rates and hence the surface of the fibre block is not perfectly flat (Fig. 30). This in turn means that the glue line can never be perfectly uniform with resulting stress distributions producing deformation of the niobate as it becomes thinner (Fig. 15b). These effects became noticeable when the niobate was less than 30 $\mu$ m thick and more marked as its thickness was further reduced. Initially fibre blocks were made with a groove 0.17mm wide but this was reduced to 0.13mm in order to reduce the glue line width and hence the resultant distortion.

### **6.3 Fabrication of the SAW Interdigital Electrode Structure**

The interdigital electrode structure was produced on the surface of the lithium niobate by a process consisting of the following steps.

1. Deposition of aluminium layer
2. Spinning on layer of photoresist
3. Exposure of pattern in mask aligner

#### 4. Etching of pattern

Deposition of the aluminium layer was carried out in a coating unit by thermal evaporation of aluminium wire which had been wrapped around a tungsten helix. The thickness of the layer, which was monitored by the use of a quartz crystal, was 300nm. It was found that cleanliness of the lithium niobate was critical to getting good adhesion between it and the aluminium. Failure to achieve this resulted in the aluminium peeling off during the photolithography or etching stages. Achieving the required degree of cleanliness is difficult because of the nature of the structure. Normal vigorous cleaning techniques such as soaking in an ultrasonic bath containing solvents is impossible since this would destroy the glue lines and result in the niobate becoming de-bonded from the fibre block. Because of the presence of the glues, the more effective solvents (acetone, dichloromethane, trichloroethylene etc) could not be used. This meant that the cleaning materials were limited to detergents (such as Decon) and the less active solvents such as isopropanol or methanol. Problems were encountered with poor adhesion, despite using as rigorous a cleaning regime as possible. It was felt that the glue surrounding the niobate and used to protect it during polishing was to a small but significant extent smearing across the niobate during cleaning. It was decided, therefore, to carefully peel off this glue prior to cleaning. This seemed to reduce the contamination but at the expense of exposing the bond line to attack during processing.

Spinning photoresist on to the device requires the utmost care since this needs to be carried out at about 3000rpm. Spinning is normally carried out on circularly symmetrical silicon wafers held by vacuum on to a chuck. To spin a silica glass block (30 x 15 x 8mm) with fibre attached, a special chuck had to be constructed. The fibre block was bonded using a UV curing epoxy on to a glass side and this slide was clamped onto the chuck. The fibres need to be carefully wound round the clamps and taped down in order to prevent them from flying off. The photoresist employed was Shipley Microposit S1818SP16.

Normally photoresist is baked at around 95°C prior to exposure in order to drive off the solvents and harden it. It was found that this baking process had a tendency to produced cracking in the niobate due to differences in thermal expansion coefficient in the structure. To overcome this problem the photoresist was left at room temperature overnight to cure. This proved to give satisfactory results provided that appropriate alterations were made to the exposure times.

Photolithography was carried out using a Kasper Quintel contact mask aligner. Guide marks were put on to the block prior to aluminisation to give an indication of the position of the interaction region so that the interdigital electrode pattern could be positioned at one end of it. A mask was ordered having various electrode designs with differing numbers and widths of electrode fingers. Unfortunately, since the mask aligner has a fluid head and the sample a very small surface area, only those patterns near the centre of the mask could be used. For patterns nearer the outside the fluid head pushed up the sample such that it was not parallel and did not make overall intimate contact with the mask. This resulted in very poor definition over part of the pattern area.

After the sample had been exposed, the photoresist was developed in Microposit developer for approximately 1 minute until the pattern was clear. If the pattern was found to be satisfactory, with good definition and "no shorts", the electrode structure was etched using a mixture of orthophosphoric acid (85%), nitric acid (5%) and water (10%). The sample was examined under a microscope to ensure that no residual aluminium was present to give a short between the electrodes. The resistance between the electrodes was also measured to back up this observation.

It is essential that very low resistance contacts are made to the interdigital electrodes in order to supply high frequency power to them. It was hoped that an ultrasonic bonder could be used to bond a gold wire to the electrodes for this purpose. As no suitable machine is available at Strathclyde University it was arranged to attempt to carry out the operation at Glasgow University. It was found, however, that the adhesion between the aluminium layer and the niobate was not sufficiently strong to permit this. When bonding was attempted the gold wire could be bonded to the aluminium but the aluminium in turn became detached from the niobate. The reason for this was probably inadequate cleanliness of the niobate prior to coating caused by problems with the cleaning procedures described previously.

Having spent a considerable time in attempting to sort out this problem without success it was decided to try an alternative method of producing contacts. This was to use sprung brass contacts on to which had been attached pads of indium. The brass contacts were mounted in a suitable jig which enabled the fibre block to be slid in under the contacts, which were then lowered to make contact with the electrode arms. The indium was abraded immediately prior to this in order to remove any oxidation on the surface which would produce a resistive layer. Resistance measurements were made to ensure that the resulting contact resistance was less than

1 ohm. It was found that the contact resistance tended to decrease in the hours after it was assembled, probably due to the malleable indium pads changing shape under pressure to give a larger contact area.

## 7. FREQUENCY SHIFTER TESTING

Once fabrication of a device is complete it is tested by wavelength scanning it by the use of a monochromator which has been adapted for fibre use. The grating used has 900 lines/cm and is rotated by means of a computer driven stepper motor. A broadband polariser is positioned between the output slit of the monochromator and the launch lens to produce linearly polarised light and a fibre polarisation controller is used to establish the required polarisation state within the device. This is necessary because the overlay will exhibit waveguide birefringence and may, depending on the orientation of the niobate being used, also have material birefringence. This means that the transmission characteristics of the device will be different from TE and TM polarisation states, with the resonances occurring at different wavelengths. It is important that the polarisation state is accurately set if the maximum depth and sharpness of resonance are to be seen.

Once the interdigital electrode structure had been successfully produced on the niobate surface, a method of detecting the effect of a SAW wave had to be considered. Frequency shifted light would be found in the niobate rather than in the fibre which meant that prism coupling or a second polished fibre block would be needed to collect it. Rather than adopt this approach it was decided to study the effect of the acoustic wave on the wavelength response of the device. In order to achieve frequency shifting the propagation constant of the light wave must be changed by a discrete amount as a result of its interaction with the acoustic wave. This in turn means that the wavelengths at which coupling may take place between the fibre and the overlay waveguide will also change. The design criteria necessary to attain SAW induced coupling at wavelengths approximately mid-way between two steady state resonant wavelengths is presented in section 4.2. The target overlay thickness was chosen to be  $25\mu\text{m}$  implying an interdigital finger spacing (i.e. SAW period) of  $87.6\mu\text{m}$  with a drive frequency of 39.7MHz to induce resonances precisely midway between the steady state positions. In practice the finger spacing was chosen to be  $80\mu\text{m}$  corresponding to a drive frequency of 43.2MHz. The criterion for achieving successful device operation was accepted as the observation of new coupling resonances approximately midway between the steady state resonances upon application of RF power to the electrodes launching the SAW.

A device having a  $24\mu\text{m}$  thick lithium niobate overlay and an interdigital electrode structure giving an  $80\mu\text{m}$  wavelength was scanned before and after the application of RF power to the electrodes. This was repeated over a wide range of frequencies

using a drive power of up to +25dBm. Unfortunately no significant variation in wavelength response was ever detected. Two examples of traces taken at 43.2MHz and 60MHz are shown in Figs. 31 and 32. Such small differences as exist between the traces are attributable to either noise or slight polarisation drift. It was therefore concluded that significant levels of frequency shifting were not being achieved.

Because of this negative result it was decided to investigate the propagation of acoustic waves in thin lithium niobate in more practical detail. In order to do this a new mask was designed which consisted of pairs of electrodes spaced 5mm apart arranged in back-to-back transmitter-receiver configuration. This electrode pattern was then produced on a thick (1mm) sheet of lithium niobate and also onto a thin (17 $\mu$ m) piece of lithium niobate bonded by LCR0001.46 adhesive on to a silica glass backing block. Power was launched to the transmitter electrodes using a high frequency signal generator and detected at the receiver pair using an oscilloscope. It was found that the power received on the 17 $\mu$ m niobate block was 28dB less than was received on the thick sample for the same input power. In order to acoustically damp the material to test for RF breakthrough a fine slurry was put on the surface of the niobate between the electrode pairs. This produced a reduction in received power of 26dB for the thick sample and 12dB for the thin layer, showing that most of the received power was due to an acoustic wave and not to RF breakthrough. The vast difference in received power between the thick and thin samples indicates that the niobate bonded onto a glass block is an acoustically extremely lossy structure. Because the thickness of the 1mm sample was so much greater than the length of the acoustic wave it could be regarded as bulk material, whereas the thin material was only about 20% of the acoustic wavelength and hence the bond layer would be extremely important. Because of the extremely lossy behaviour of the epoxy used it was hoped to replace it with the more acoustically suitable phenyl salicylate. However, as described in Section 6.2 this was found to be impractical due to bond failure during the lapping process.

It was concluded that the failure to see any change in the transmission characteristics of the device as a result of the applied RF power was due to the very high attenuation of the SAW wave by the epoxy bond layer. No other bonding material has been found which has the desired combination of acoustic and optical properties. The ringing on method would appear to be ideal but only if the epoxy bonding the fibre into the block could be replaced by a glassy material and thus remove the weaknesses at these points. The alternative approach would be to find some suitable material and directly apply it to the fibre block surface by some deposition technique. It is not at

all clear as to what a suitable material might be and it would require a major research program to learn how to achieve the necessary material properties. PLZT or ZnO may be suitable candidates.

Before attempting to fabricate any further acoustic wave structures it was decided to investigate the effects of a stationary electro-optically induced refractive index grating in the niobate overlay. It was hoped that this would give an indication of the amount of refractive index change which would be necessary to cause a change in the device transmission. This in turn would indicate whether an acoustic wave could give changes of the required order of magnitude. In order to do this a new mask was designed having an electrode pattern 4mm long, which could cover the entire interaction region. This pattern consisted of 20 $\mu$ m wide fringes with equivalent spacings between them. Instead of positioning this electrode pattern away from the interaction region it was positioned directly above it.

In order to optically isolate the waveguide from the metal electrodes it was necessary to incorporate a 300nm thick low index ( $n=1.39$ ) magnesium fluoride buffer layer which was evaporated onto the niobate surface before the aluminium for the electrodes was added. The device was tested in the same manner as the ac devices except that a dc power supply was used giving up to 100V potential. The applied voltage was increased in steps from 10V to 100V with a wavelength transmission scan being carried out at each value. No significant difference could be determined between any of these scans, any small discrepancies being found to be due to noise or polarisation drift (Figs. 33 and 34). Having carried out these experiments the sample was inspected under a microscope where damage due to electrical breakdown was seen to have occurred (Fig 35). Each alternate finger had a "nibbled" appearance along that part of its length which was nearest the next electrode. A further layer of magnesium fluoride was deposited on to the electrode (but excluding the contact pads) in order to prevent this from happening. The wavelength scans were repeated as before at various voltages but again no differences could be found. A mathematical analysis of the fields to be found inside the niobate is shown in fig 36. It would be expected that only the TM component would respond to the application of this dc field since there would be no change in index in the direction of the electric field of a TE wave. During these experiments the polarisation state was carefully established and scans carried out for each. However, as stated above no change was ever detected. The reason for this remains unclear, though electrode damage due to breakdown may have caused a problem. It is hoped to repeat this experiment at a later date and any significant progress will be notified to AFOSR.

Attempts were also made to fabricate the Bragg frequency shifter. However, the higher acoustic frequency, 500MHz, and the corresponding finer IDE pattern (finger spacing  $<5\mu\text{m}$ ) only served to compound the fabrication difficulties. As a result all attempts to realise a device within the timescales of the programme were unsuccessful.



## 8. WAVELENGTH SELECTIVE ELEMENTS

The basic wavelength response of a fibre optic overlay device structure is that of a channel dropping filter (Figs.16 & 23)<sup>20</sup>. The spacing between resonances is controlled by the overlay thickness and, in general, it can be arranged that only one resonance occurs in any particular range of interest. At the resonant wavelength power couples into the overlay where it is available for direct transfer to an optical receiver via high index output coupling or further coupling to a second fibre. Such devices are of great interest in a wavelength division demultiplexing role to select a single wavelength channel from a fibre with high resolution ( $<2\text{nm}$ ) and couple it to a receiver whilst all other channels are transmitted down the signal fibre with low loss ( $<0.2\text{dB}$ ). The work reported here has shown that filter linewidths down to a few nanometres<sup>20</sup> may be realised and coupling efficiencies of up to 75% may be achieved for the selected wavelength. Furthermore, if the overlay is formed of electro-optic material addressed by a suitable electrode structure the selected wavelength may be tuned by application of a variable voltage<sup>20,21</sup>. This has been demonstrated using lithium niobate<sup>21</sup> in a device structure which required about 100V per nanometre of tuning. A simple calculation, however, shows, that for strontium barium niobate in the role of the overlay, tuning efficiencies of around 1-2V/nm may be achieved and with liquid crystals even better figures are possible. Furthermore large tuning ranges ( $>100\text{nm}$ ) are available by variation of the superstrate index<sup>22</sup>.

The cross coupled arm of the switching structure exhibits a pass band filter response (Fig.27 & 28). In addition, within another programme at Strathclyde a modified version of a simple overlay structure has been shown to yield a tunable pass band response. Such devices have applications in WDM systems, in filtering of the output of optical amplifiers and in the wavelength selection and control of fibre lasers. Indeed such a filter has been used in the cavity of an erbium doped fibre ring laser to achieve tunable single mode operation with an output linewidth in the region of 100kHz.

## 9. CONCLUSIONS

An extensive development programme has been carried out to realise an in-line fibre optic frequency translator based on surface acoustic wave (SAW) interaction with the optical coupling from a side polished single mode fibre to a planar waveguide overlay. This work included the comprehensive development and characterisation of fibre optic overlay device structures and a targeted fabrication exercise to realise the frequency shifter. To form the acousto optic overlay waveguide the only realistic approach available to us was to use lithium niobate bonded to the polished fibre block and subsequently polished to the required thickness. Many problems had to be solved regarding the parallelism of the overlay and its mechanical integrity (it tended to crack) during the polishing process. Furthermore, the photolithographic processes to realise the SAW interdigital electrode pattern often led to detachment of the bonded overlay due to the harsh processes involved (i.e. baking, chemical etching etc). Essentially the fabrication procedure is laborious and involves many risky and difficult processes requiring highly skilled personnel. As a consequence the yield was low with often many weeks of painstaking effort required to realise a single device. Indeed, several complete devices were only realised during the last three months or so of the main programme and during the six month extension. However, despite exhaustive tests and a number of design iterations, no evidence of frequency shifting was found.

At this point an experiment was set up to compare the efficiencies of a launch/receive system on bulk lithium niobate with that of a thin polished layer bonded to a glass support disc. The efficiency of the latter was about three orders of magnitude down on the former thus identifying the basic problem. This was surprising since the bonding layer is only about  $1\mu\text{m}$  or so thick. Obviously the acoustic properties of the bonding agent are such that the SAW is severely attenuated. An alternative bonding medium (phenyl salicylate) with better acoustic properties was investigated but it could not survive the polishing process.

In view of the above we conclude that fibre optic overlay frequency shifters fabricated by the approach adopted here would have very low efficiency and would not lend themselves to ease of manufacture. If the overall principle of frequency shifting using the fibre optic overlay approach is to be further investigated then acousto-optic overlays should be fabricated by vacuum deposition of active material (e.g. PLZT or ZnO) directly onto the polished fibre. Alternatively, slivers of lithium niobate may be rung to the surface of the fibre block but considerable development of the polished

fibre block would be required to achieve an all glass structure.

On a more positive note the frequency shifter programme has resulted in the development and characterisation of fibre optic overlay devices as wavelength selective elements. Devices in the configuration of channel dropping filters and band pass filters have been realised and the principles of tuning by electro-optic variation of the superstrate or overlay refractive index have been demonstrated. Filter linewidths down to a few nanometers have been achieved with losses of less than 0.2dB for the channel drop structure and less than 2dB for the band pass configuration. Such devices have extensive applications in fibre optic technology including wavelength division multiplexing, filtering (e.g. of optically amplified signals), optical sensing (e.g. pH, chemical and environmental sensing) and wavelength selection and tuning in fibre lasers. Outwith this programme a band pass filter has been used within the cavity of an erbium doped fibre ring laser to provide single mode output (linewidth  $\sim 100\text{kHz}$ ) tunable over the full  $\text{Er}^+$  fluorescence spectrum.

As regards the optical isolator it was found that the only material with a sufficiently high Verdet constant was Bismuth Iron Garnet which was only available in 2mm square by  $300\mu\text{m}$  thick samples epitaxially grown on a GSGG substrate. The cost per sample was  $>\$1000$  and the most efficient magneto optic axis was perpendicular to the film (we need it parallel to the plane of the film). Attempts were made to fabricate a device as depicted in Figure 6. However, the handling problems associated with the bonding and polishing of such small samples of the wrong crystalline orientation precluded the realisation of anything useful. In view of these difficulties it was decided to terminate work on the isolator by mutual agreement with the project monitor (see May 1992 quarterly report).

WJ/GT

April 1993

**REFERENCES**

1. C A Millar, M C Brierley and S R Mallinson, "Exposed core single mode fibre channel dropping filter using a high index overlay waveguide" *Optics Letters* **12**, 4, 284, 1987
2. R Bergh, C Kotler & H J Shaw, "Single mode fibre optic directional coupler" *Electronic Letters* **16**, 7, 260, 1980
3. W Johnstone, G Stewart, T Hart and B Culshaw "Surface Plasmon Polaritons in Thin Metal Films and their Role in Fibre Optic Polarising Devices", *J Lightwave Technology* **8**, 4, 538, 1990
4. P Yeh, "Optical Waves in Layered Media" Wiley, 1988
5. A Korpel, "Acousto-optics: A Review of Fundamentals" *Proc. IEEE* **69**(1) Jan 1981, pp48-53
6. P Debeye, F W Sears "On the Scattering of Light by Supersonic Waves" *Proc. Nat. Acad. Science (US)* vol. 18, pp409-414
7. R Adler "Interaction Between Light and Sound" *IEEE Spectrum* vol. 4, pp42-53, 1967
8. C Stewart et al "500 MHz Bandwidth Guided Wave L-band Bragg Cell" *Electronics Lett.*, vol.17(25), pp971-973, 1981
9. C Tsai "Guided Wave Acousto-optic Bragg Modulators for Wide Band Integrated Communications and Signal Processing" *IEEE Trans. Circ. Syst. CAS-26*(12), pp1072-1098, 1979
10. W R Klein, B D Cook "Unified Approach to Ultrasonic Light Diffraction" *IEEE Transactions on Sonics and Ultrasonics*, SU-14(3) 1967, pp123-134
11. W R Smith et al "Analysis of Interdigital Surface Wave Transducers by use of an Equivalent Circuit Model" *IEEE Transactions on Microwave Theory and Techniques* MTT-17(11) 1969, pp856-864
12. W R Smith et al "Design of Surface Wave Delay Lines with Interdigital Transducers" *IEEE Transactions on Microwave Theory and Techniques* MTT-17(11) 1969 pp865-873
13. D Marcuse "Directional Couplers Made of Non-Identical Asymmetric Slabs" *Journal of Lightwave Technology* LT-5(2)87 pp268-273
14. Y Cheu, S Snyder "Grating Assisted Couplers" *Optics Lett.* **16**(4) pp217-219

15. P L Chu, A Snyder "Theory of Twin Core Optical Fibre Frequency Shifter:"  
Electronics Lett. 23(21), pp 1011-1012, 1987
16. W P Risk et al "Acousto-optic Frequency Shifting in birefringent Fibre"
17. W P Risk "Tunable Optical Filter in Fiber-optic Form" Optics Letters Vol.11(9),  
1986, pp578-580
18. H Engan, T Myrveit, J Askautrud, " All Fibre Acousto-optic Frequency Shifter  
Excited by Focused Surface Acoustic Waves" Optics Letters 16(1), pp24-26, Jan  
1991
19. P Greenhalgh, A P Foord, P A Davies "Fibre Optic Frequency Shifters" FO90, pp5-  
51-5-62
20. W Johnstone et al "Fibre Optic Wavelength Channel Selector with High Resolution"  
Electronic Letters, 28, 14, 1364, 1992
21. W Johnstone et al "Fibre Optic Modulators using active Multimode Waveguide  
Overlays" Electronic Letters 27, 11, 894, 1991
22. W Johnstone et al "Fibre optic refractometer using multimode waveguide overlay  
devices" Optics Letters, 17, 21, 1538, 1992

TABLE 1: Design Criteria for Fibre Bragg Frequency Shifter.

$f_0$ (MHz)	$Q$	$\lambda_a$ ( $\mu\text{m}$ )	$L$ ( $\mu\text{m}$ )	$\alpha_B$ (Degrees)	Beam Width ( $\mu\text{m}$ )
	$2\pi\lambda L/n\lambda_a^2$		$2n\lambda_a^2/\lambda$	$\sin^{-1}(\lambda/2n\lambda_a)$	$L\sin\alpha_B$
500	$4\pi$	7.0	168	2.38	7.0
400	$4\pi$	8.7	260	1.90	8.7
300	$4\pi$	11.6	462	1.44	11.6
200	$4\pi$	17.5	1050	0.98	17.5
100	$4\pi$	34.9	4170	0.48	34.9

TABLE 2: Approximate Centre Frequency for Off Resonance Coupler Operation

Overlay Thickness $d$ ( $\mu\text{m}$ )	$\delta n/2$ (Off Resonance)	$\Delta\beta$ $\times 10^3$	Drive Frequency MHz
5	0.0736	355	197
10	0.0368	178	98.7
15	0.0245	118	65.5
20	0.0180	87	48.2
30	0.0123	54	30.1

$\lambda = 1.3 \mu\text{m}$ ,  $n_2=2.2$ ,  $n_e = 1.456$

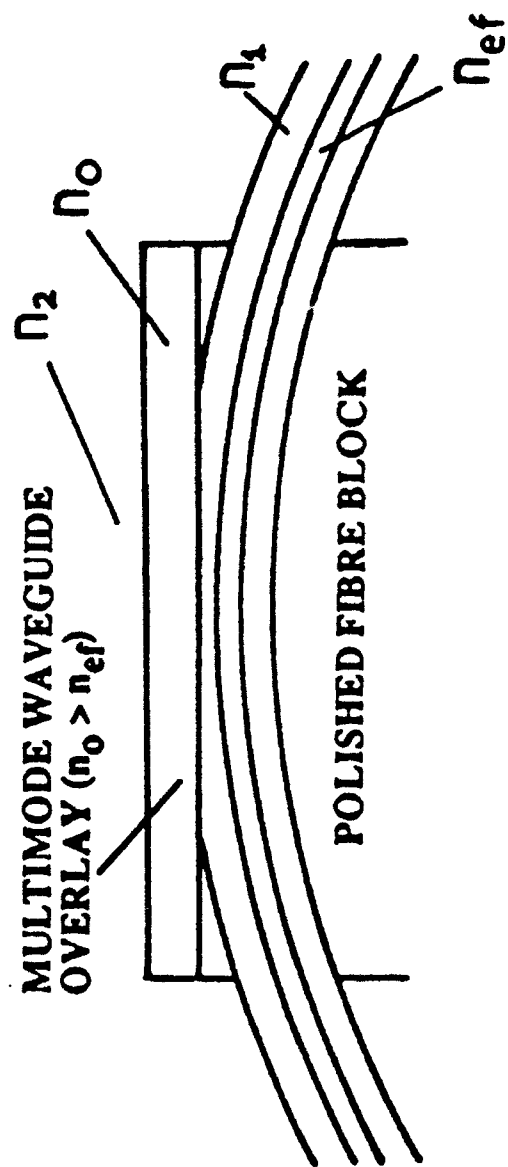


**Figure 1 :** Schematic diagram of basic device structure: side polished fibre with multimode overlay



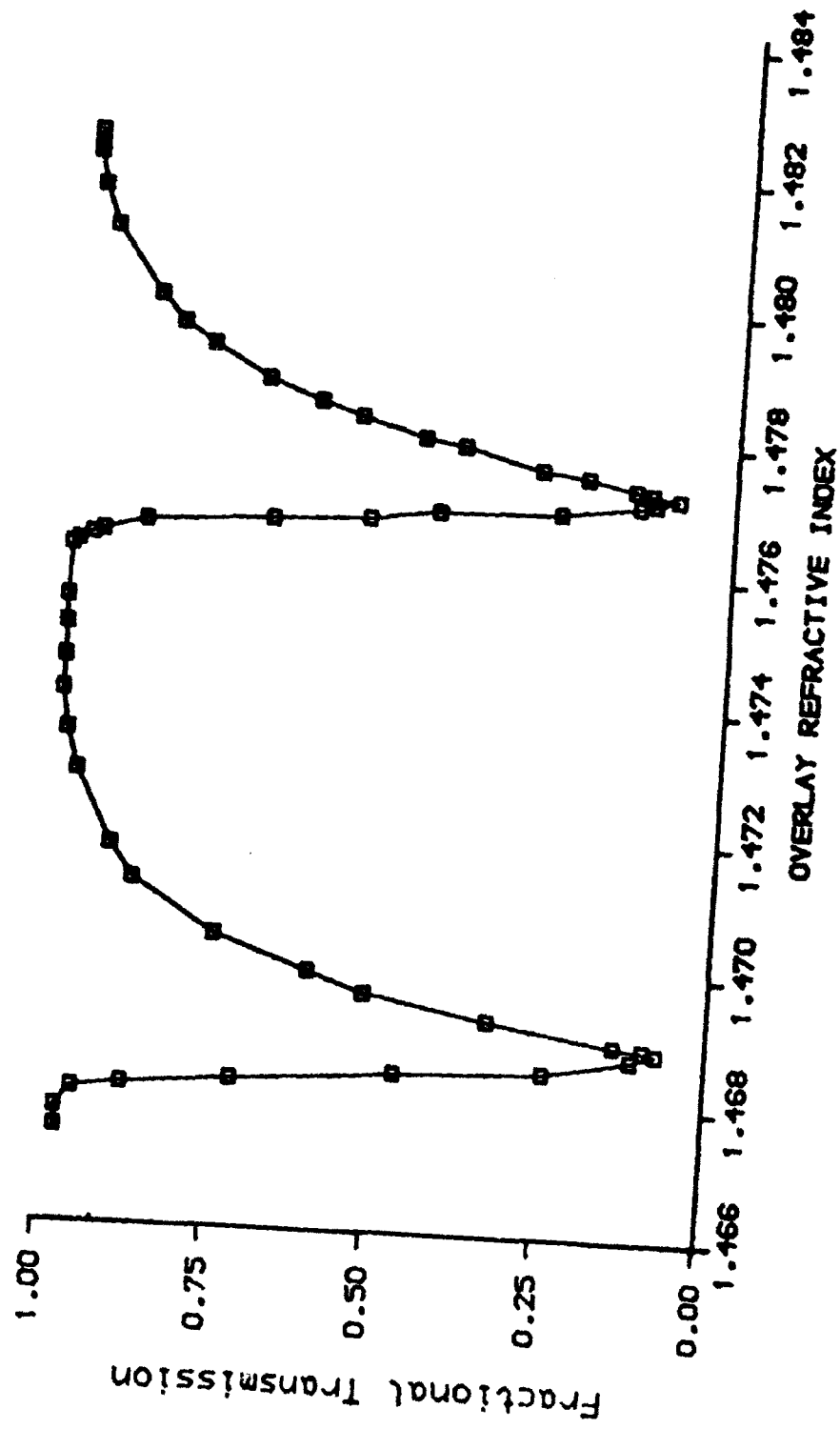


Figure 2: Fractional transmission variation with overlay index

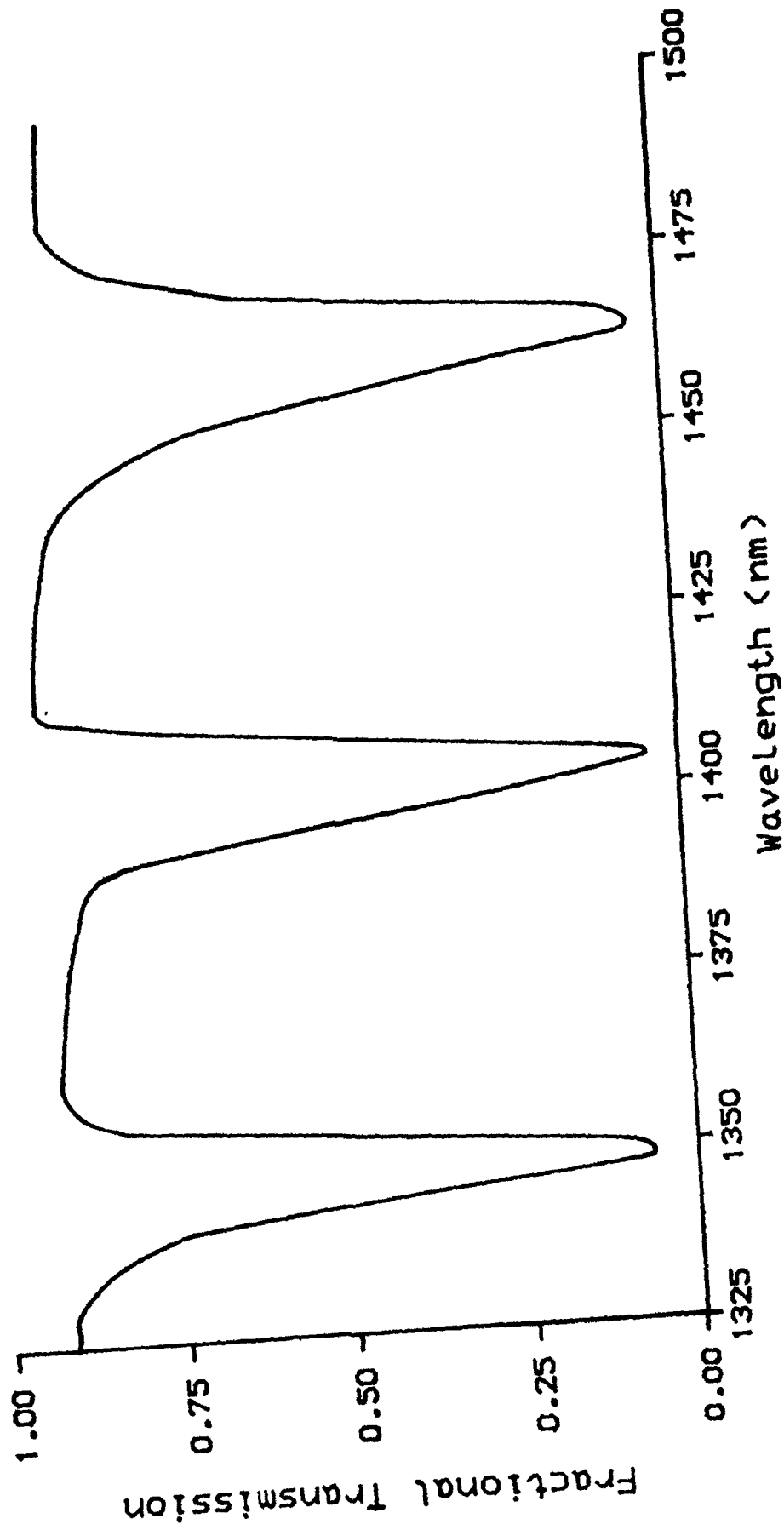
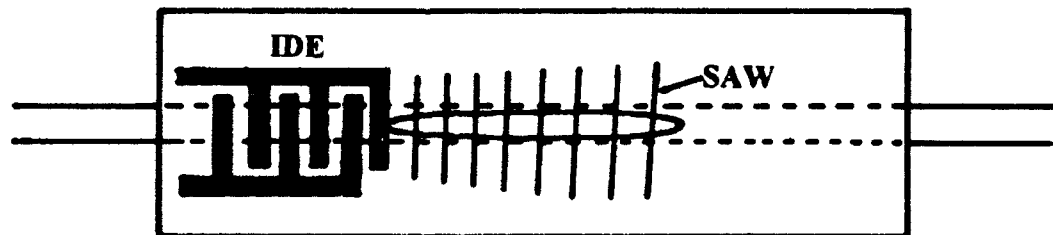
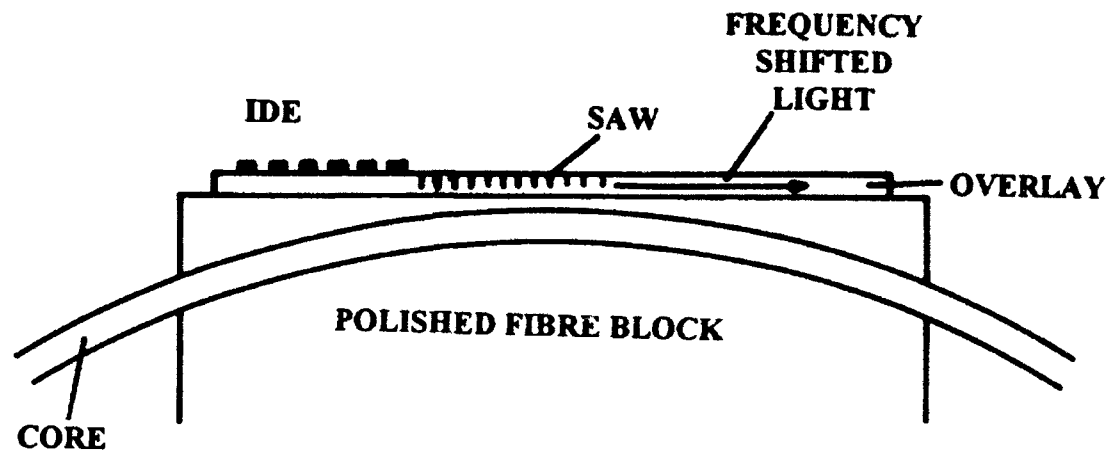
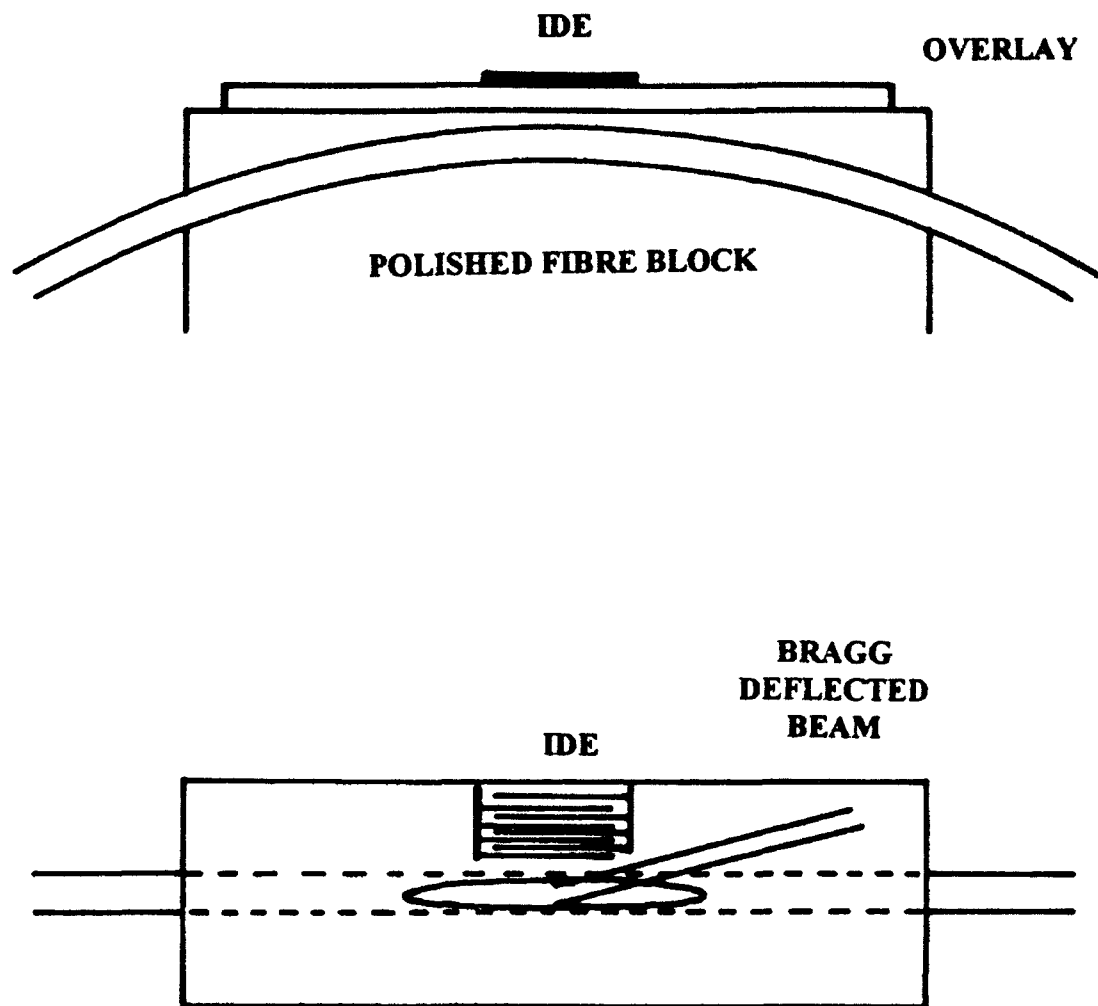


Figure 3: Fractional transmission variation with wavelength



**Fig. 4** Acousto optic frequency shifter based on modulation of the coupling from the fibre to the overlay



**Fig. 5**      **Acousto optic Bragg frequency shifter**

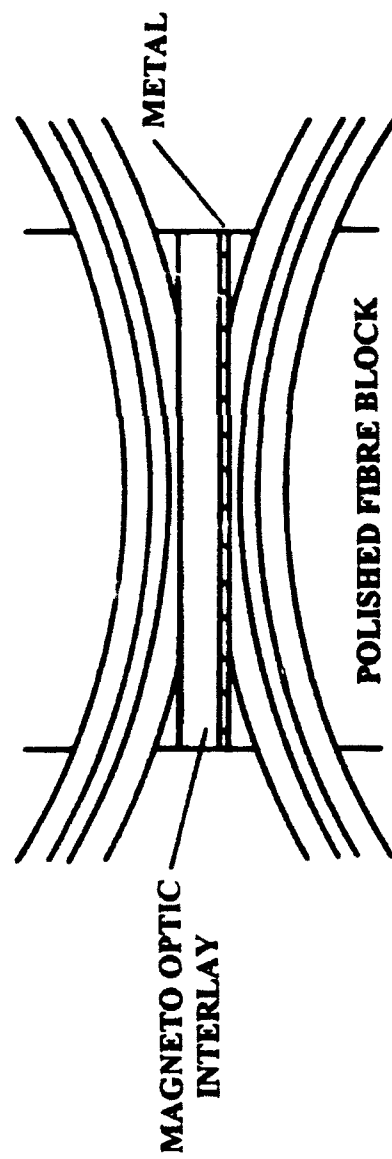


**Fig. 6** Schematic diagram of proposed optical isolator

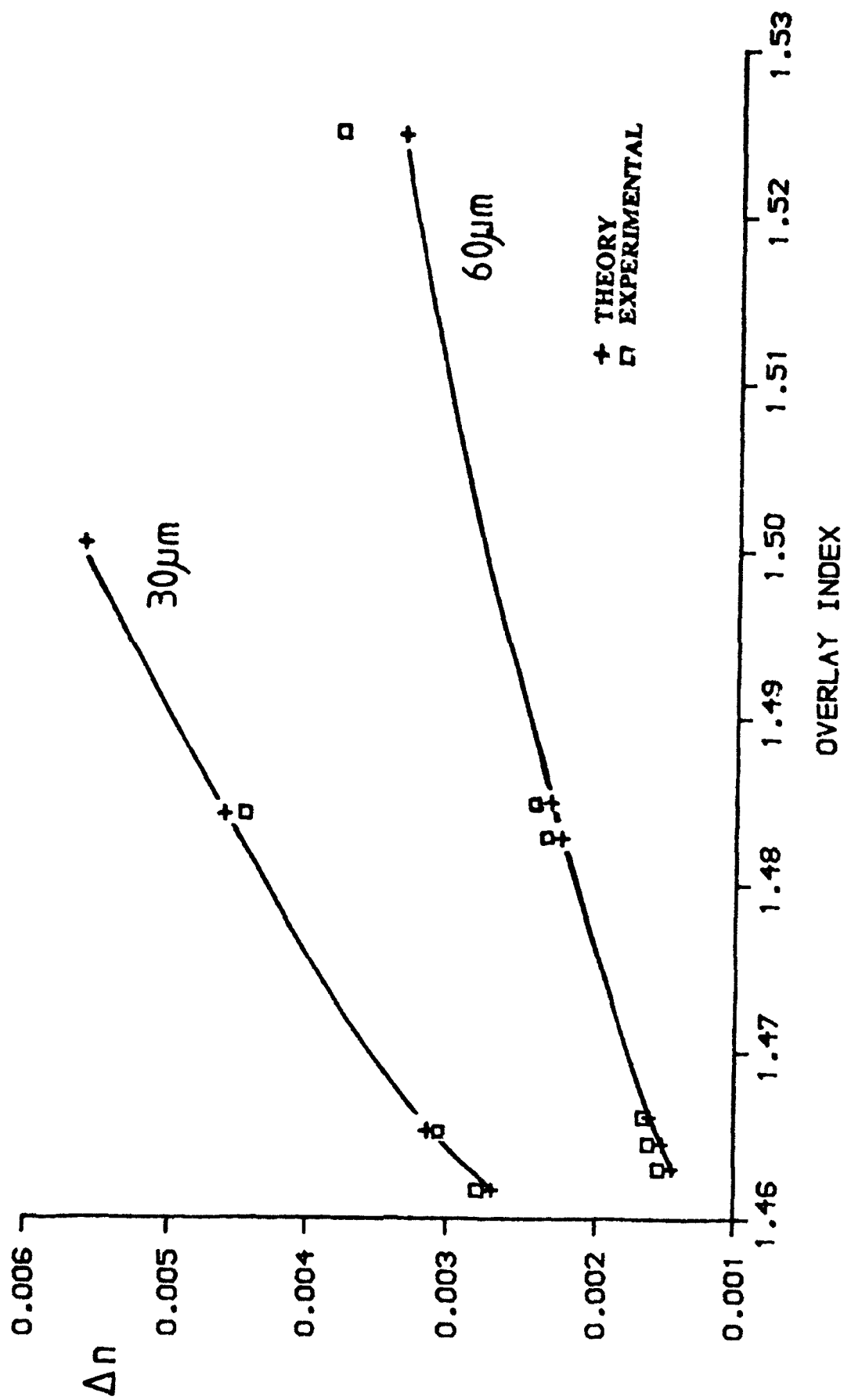


Figure 7  $\Delta n$  versus overlay index at thickness 30  $\mu\text{m}$  + 60  $\mu\text{m}$

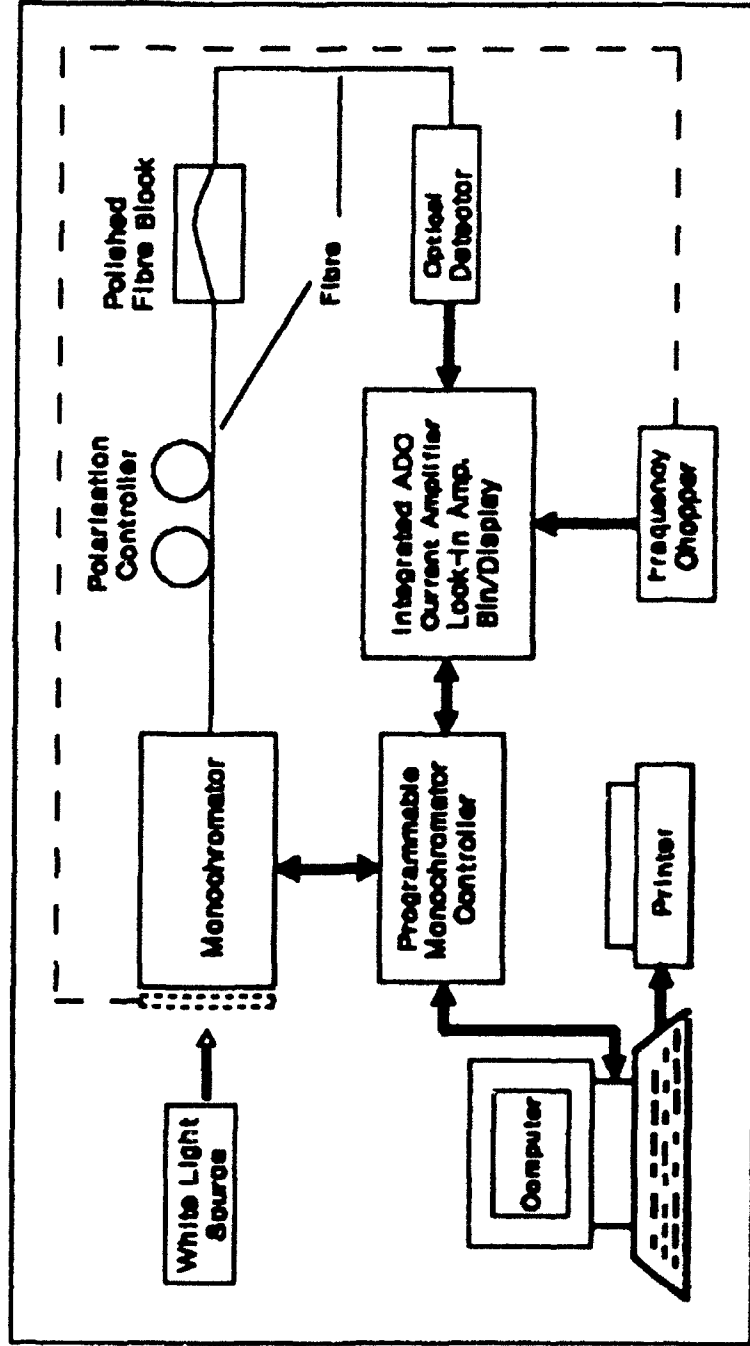
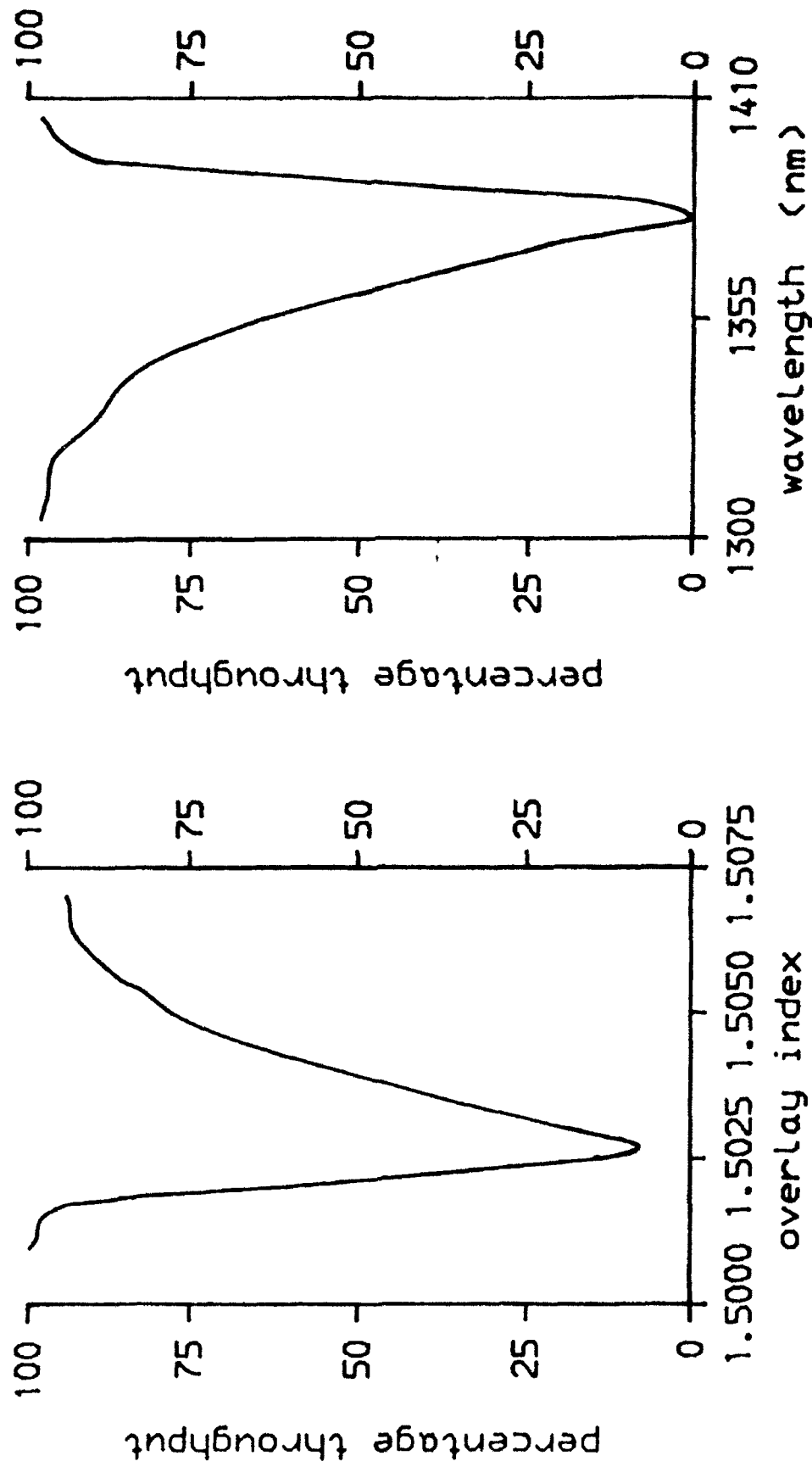


Fig. 8 Experimental System for the measurement of wavelength responses



**Figure 9** a) Thermally induced index response

b) Wavelength response for 23μm thick overlay oil ( $n_o = 1.504$ )



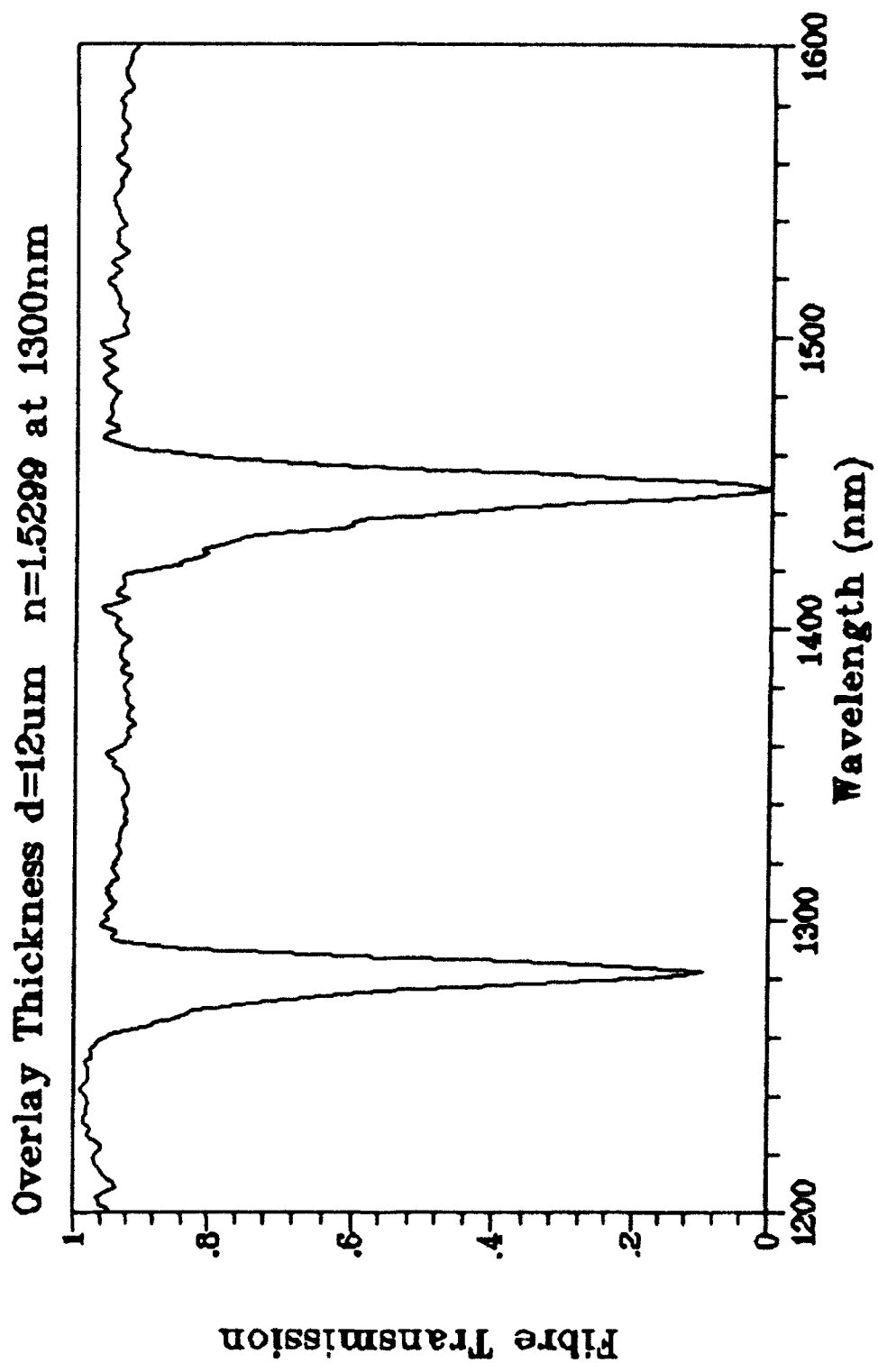


Figure 10 Wavelength Response of Oil Overlay

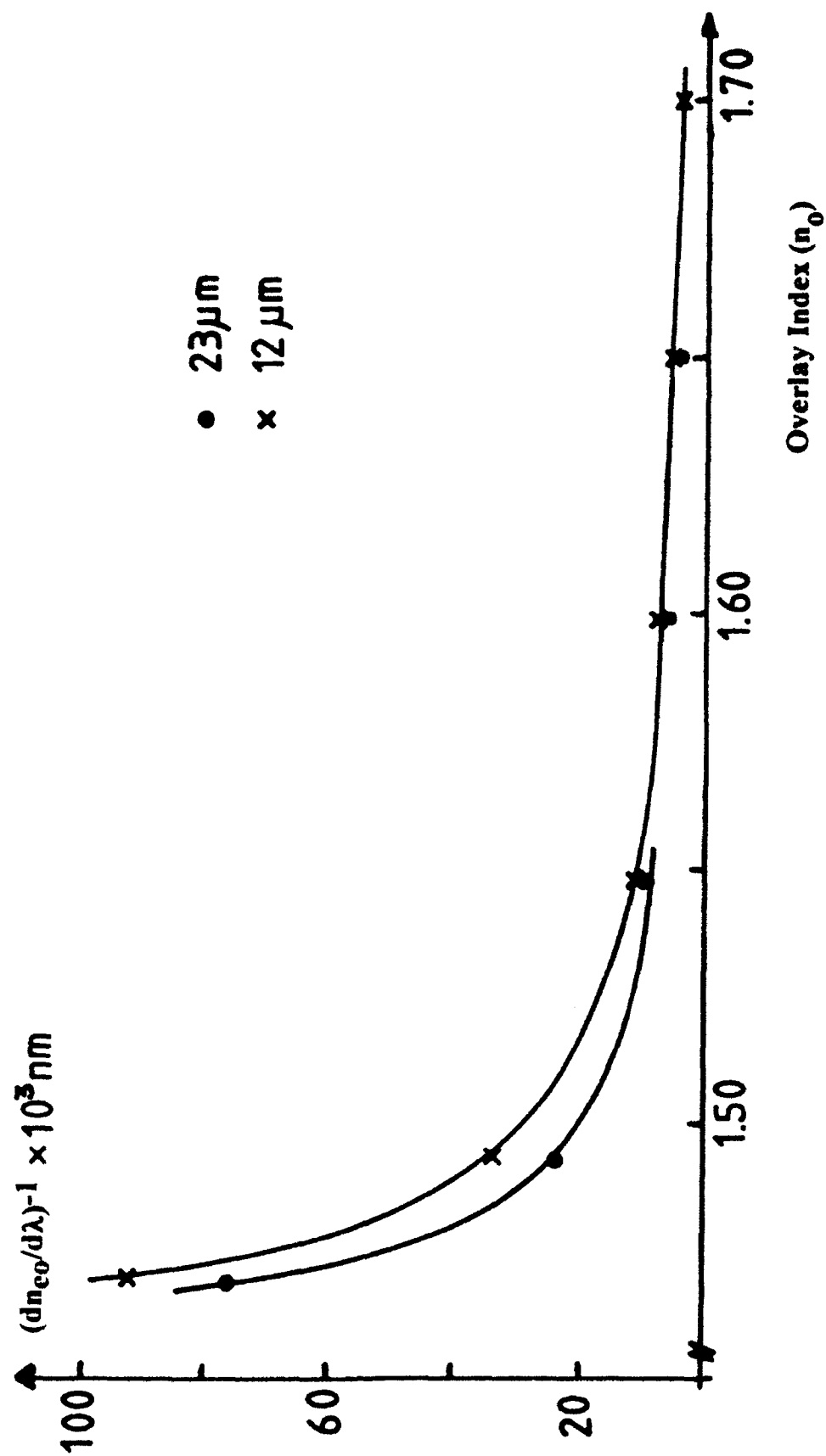


Fig. 11  $(dn_{eo}/d\lambda)^{-1}$  versus overlay index for 12μm and 23μm thick overlays

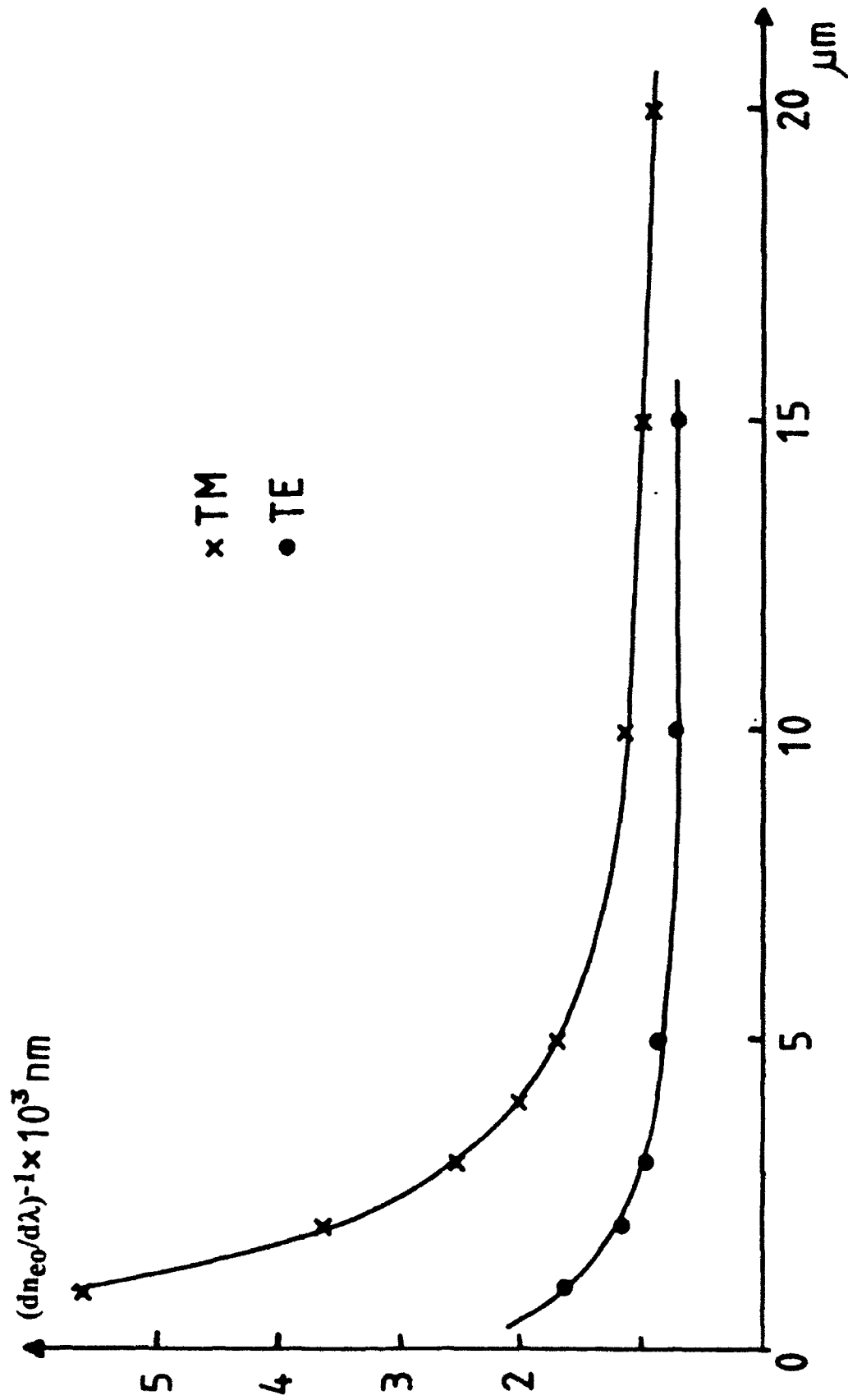


Fig. 12  $(dn_{eo}/d\lambda)^{-1}$  versus thickness,  $d$ , for lithium niobate overlays ( $n_o = 2.2$ )

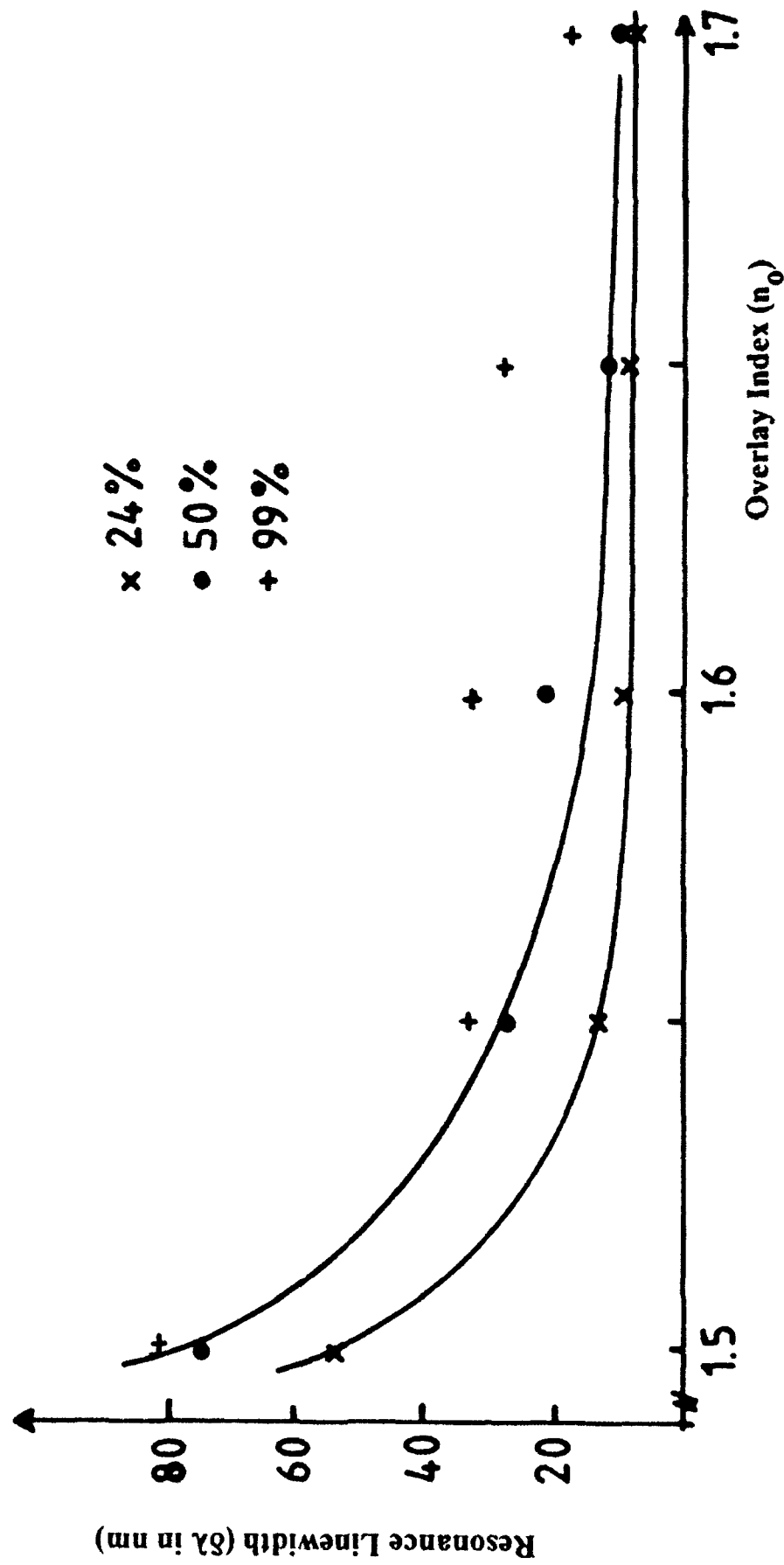


Fig. 13 Measured linewidth,  $\delta\lambda$ , versus  $n_0$  for 24%, 50% and 98% coupling block for  $d = 12\mu\text{m}$

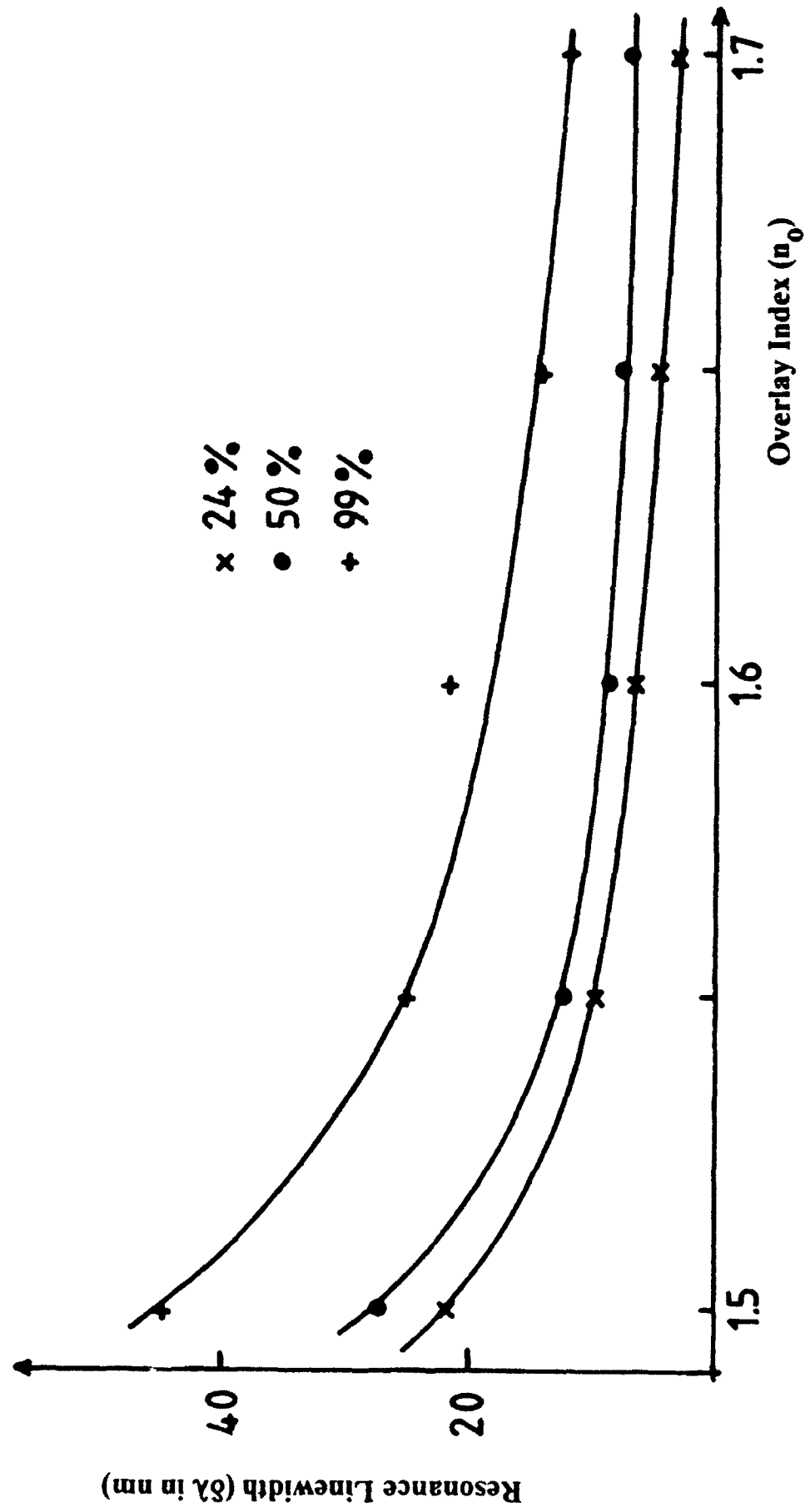
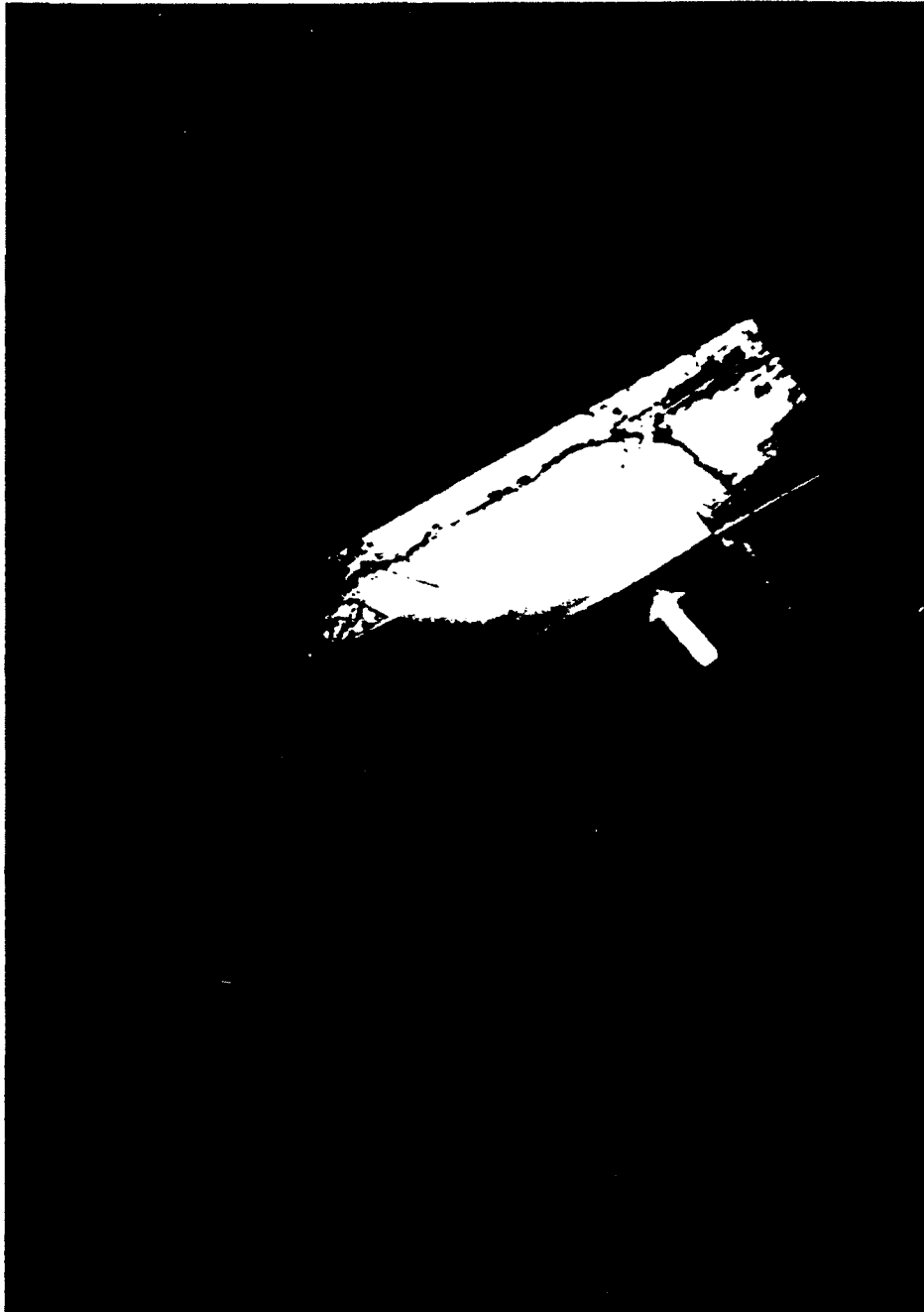


Fig. 14 Measured linewidth,  $\delta\lambda$ , versus  $n_0$  for 24%, 50% and 98% coupling block for  $d = 23\mu\text{m}$



**Figure 15a**



**Figure 15b**

**The arrow indicates distortion of the overlay  
due to the presence of the glue line beneath it.**

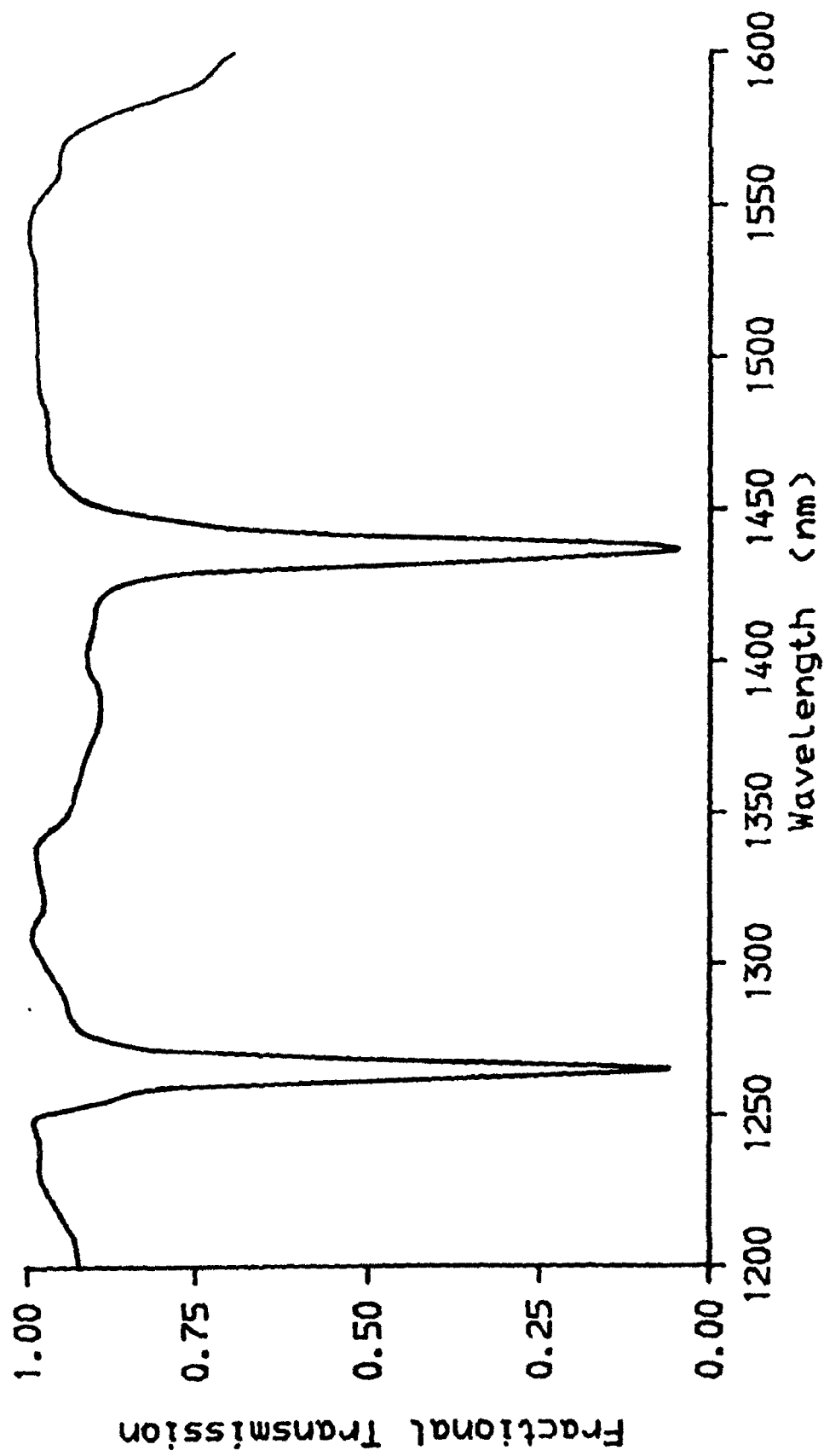
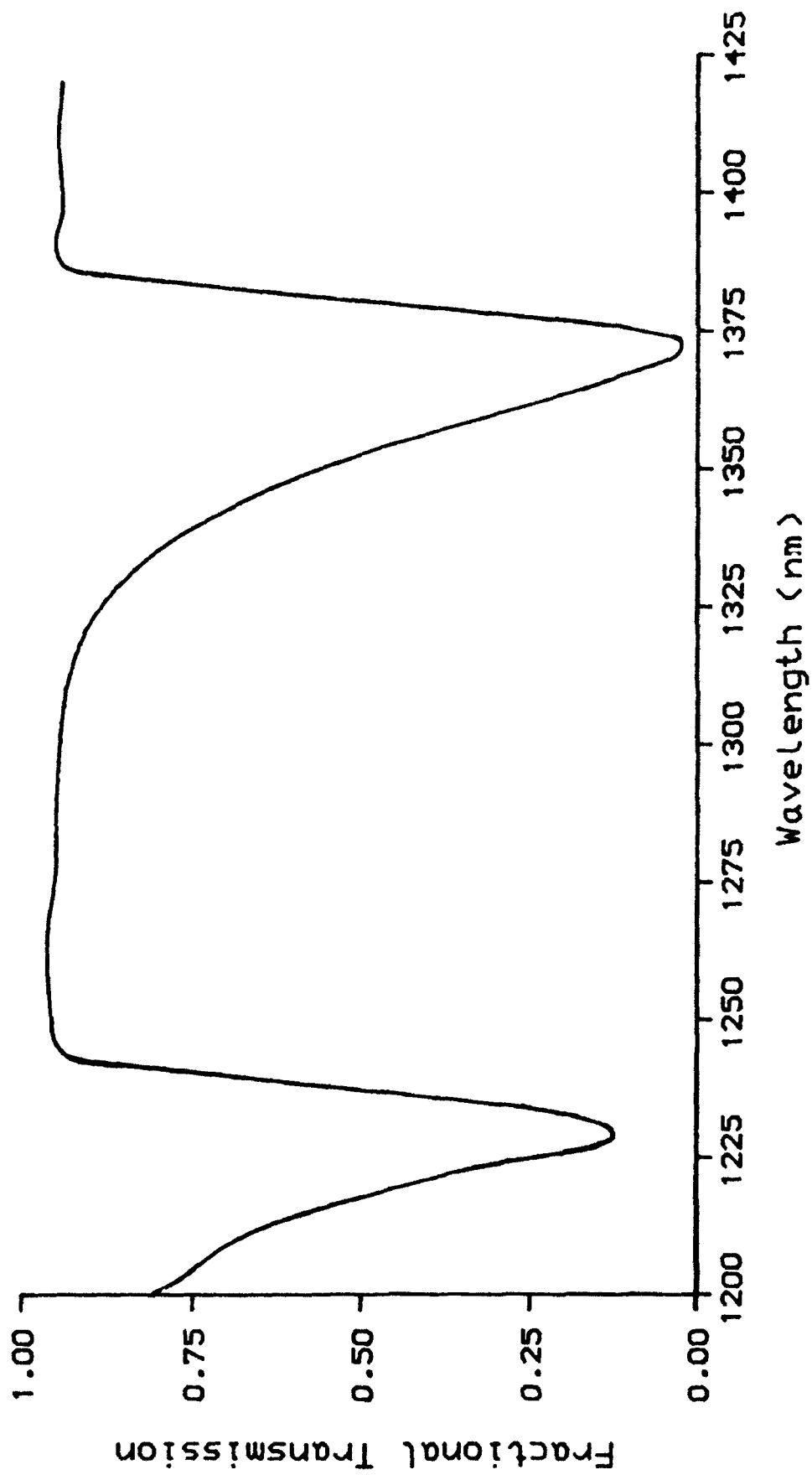


Figure 16. Wavelength response of a device using a 2.5 $\mu$ m zinc selenide overlay





**Figure 17. Wavelength response of a device using a 27 $\mu$ m BK7 overlay**

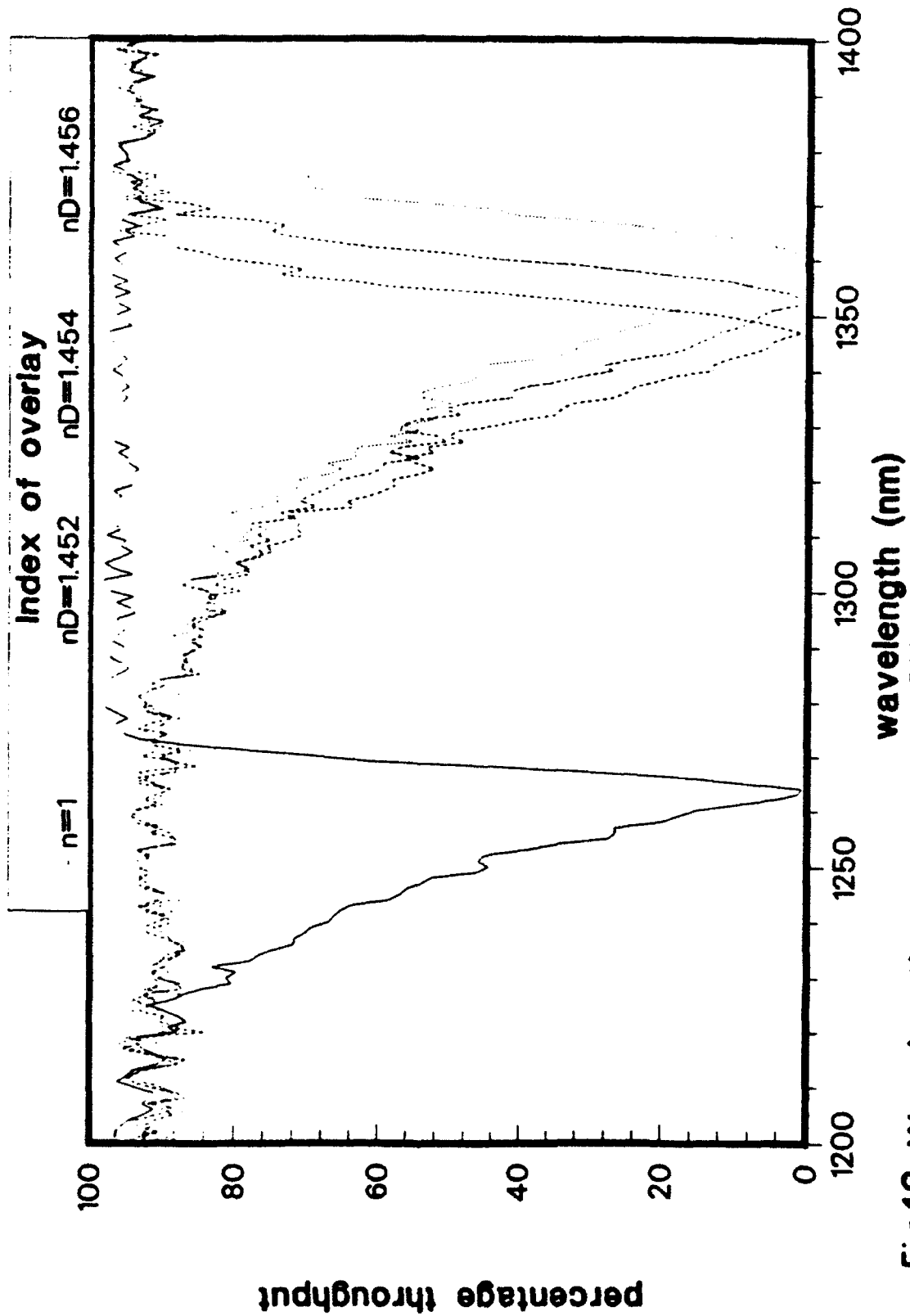


Fig18. Wavelength response of BK7 device,  $d=7.25\mu m$

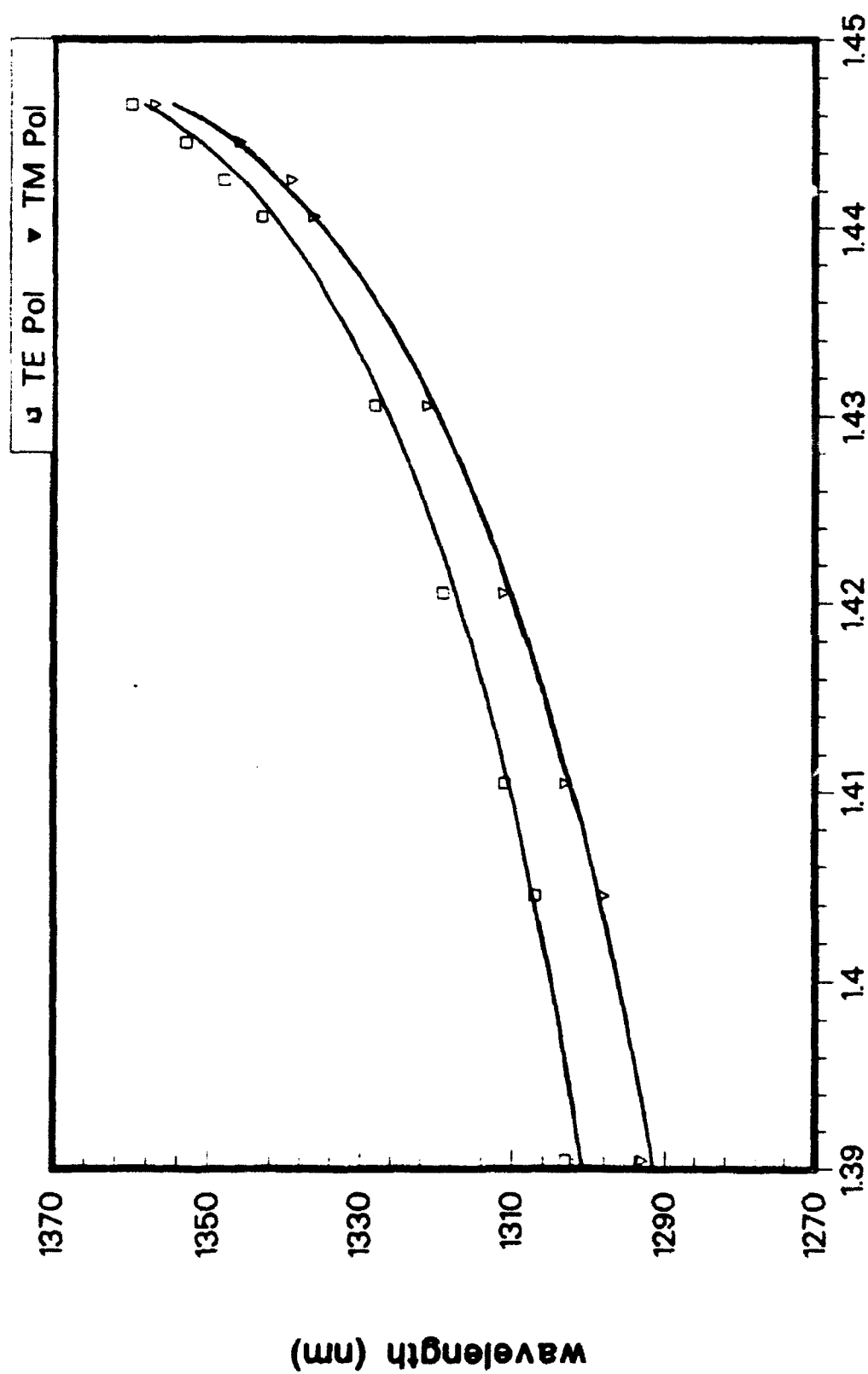


Fig19. Resonance position with superstrate index for  
BK7 overlay ( $d=7.25\mu\text{m}$ )

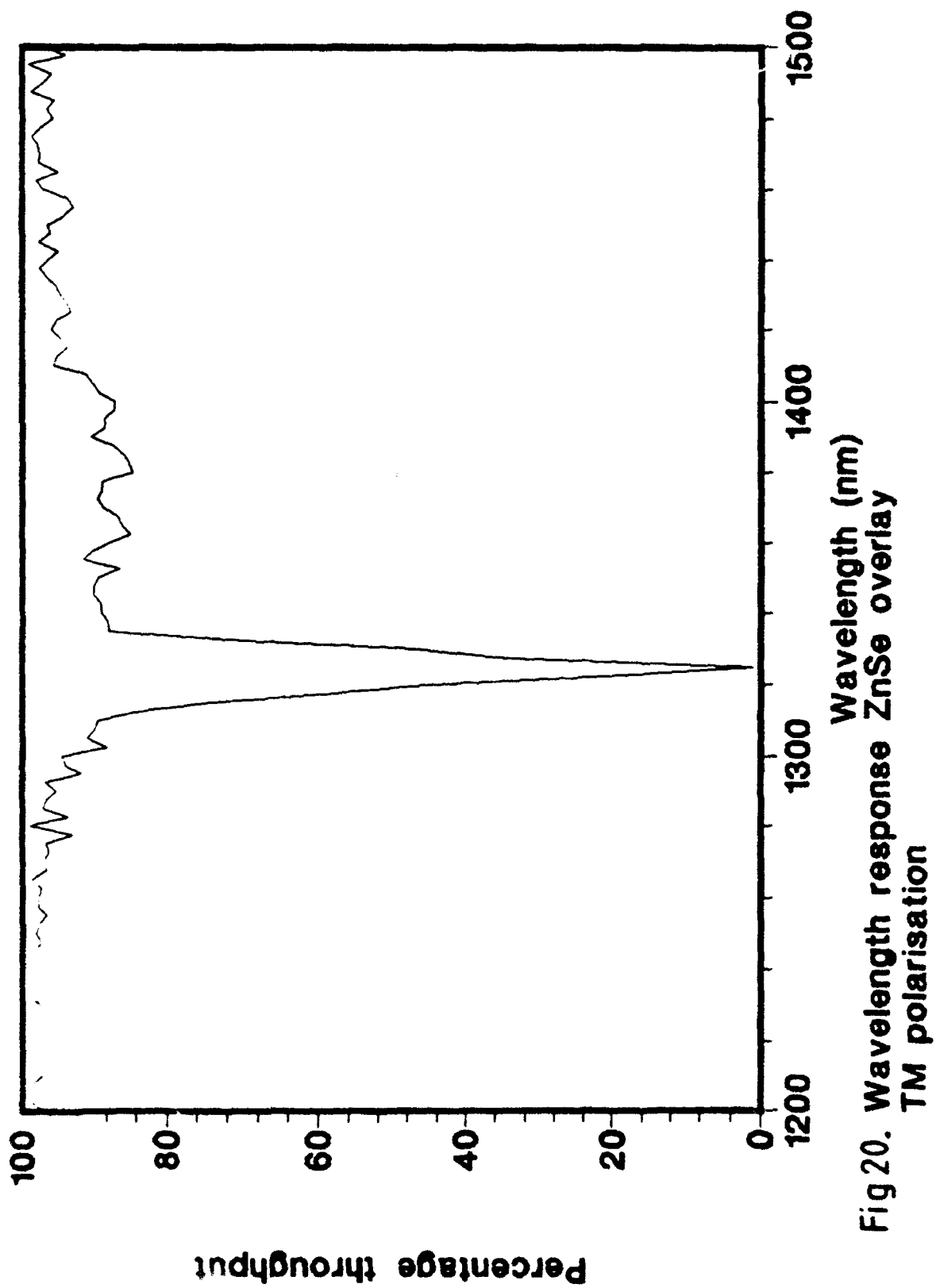


Fig 20. Wavelength response ZnSe overlay  
TM polarisation

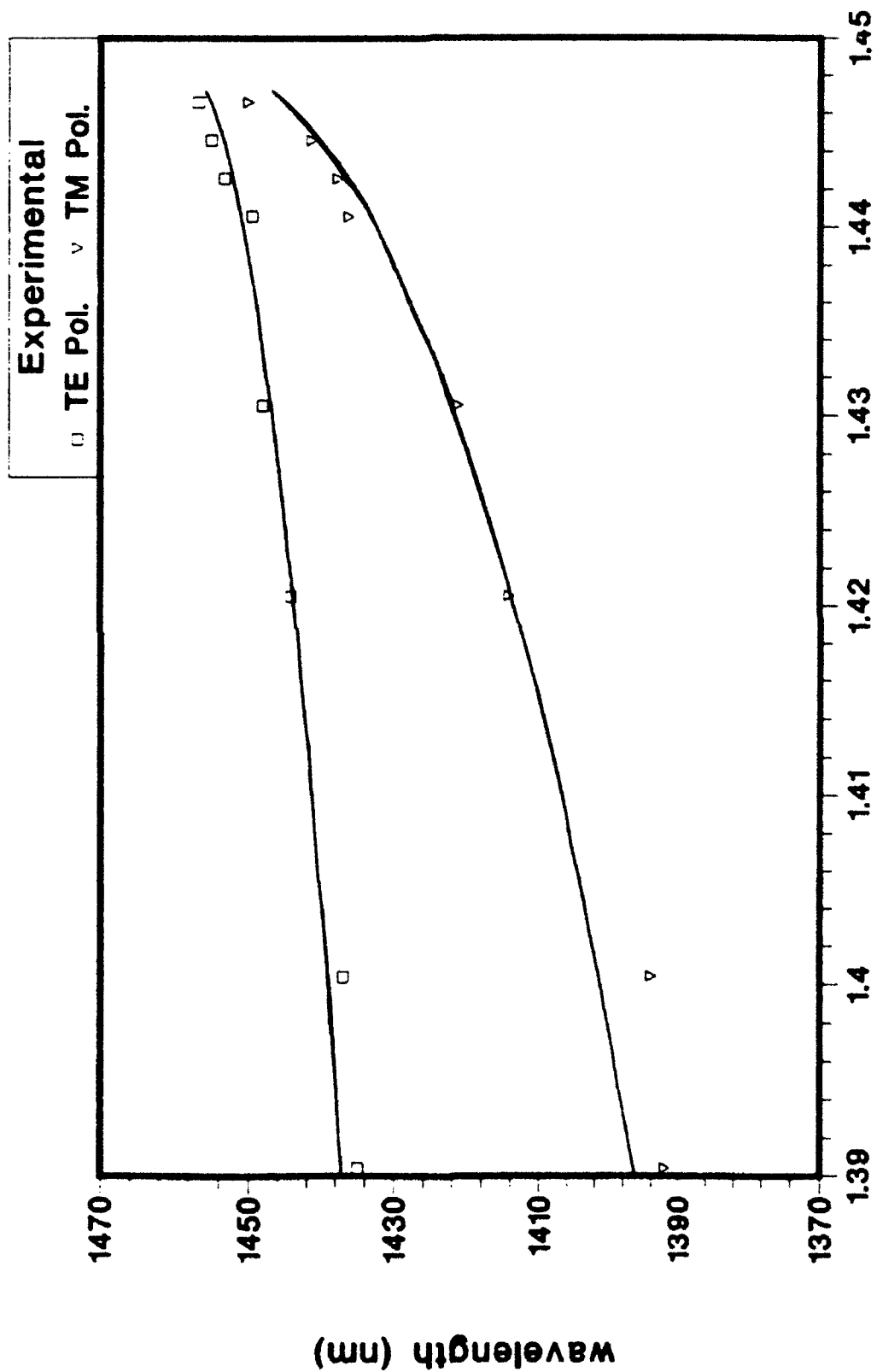


Fig21. Resonance position with superstrate index for ZnSe overlay (d=1.5um)

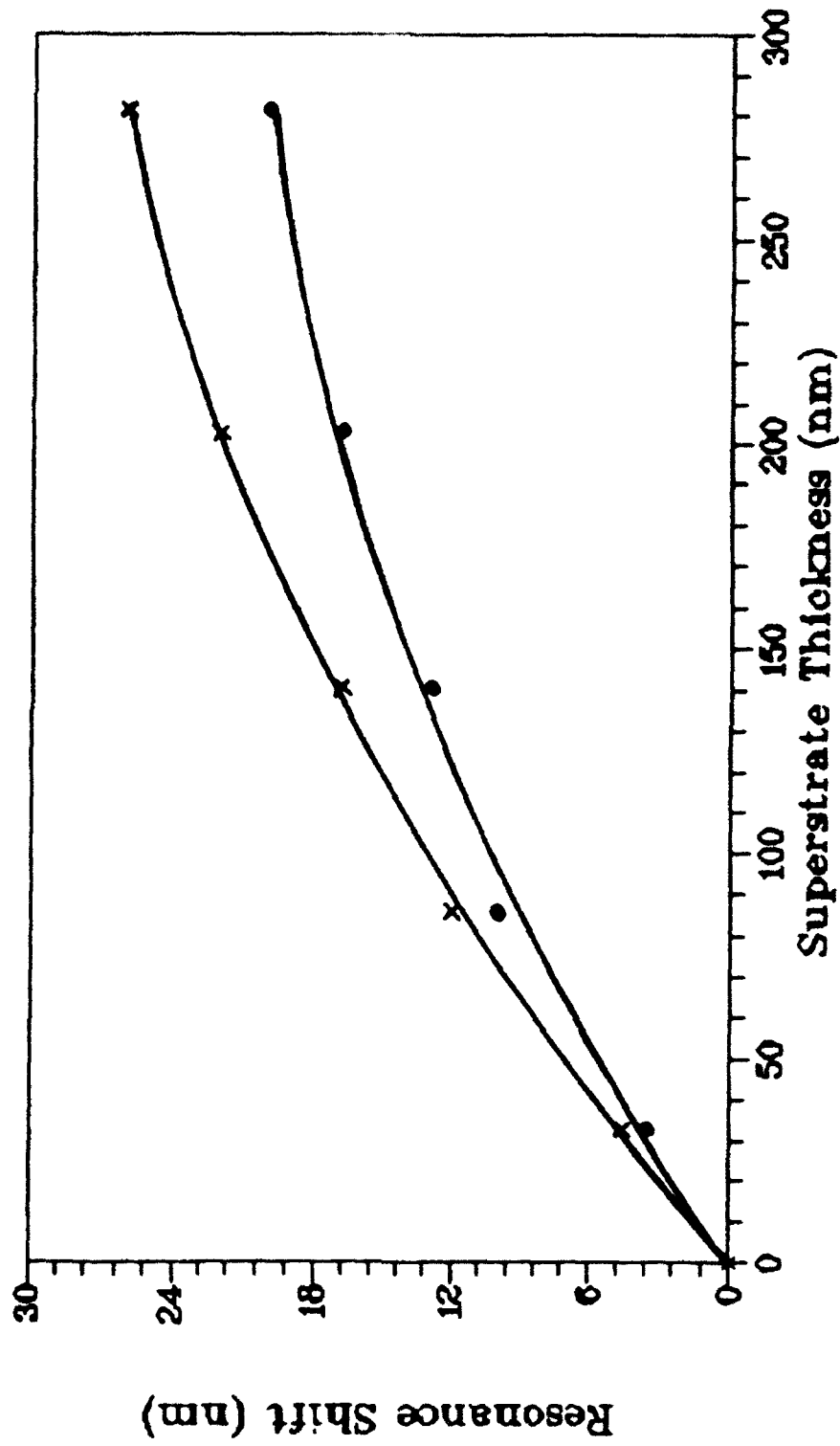
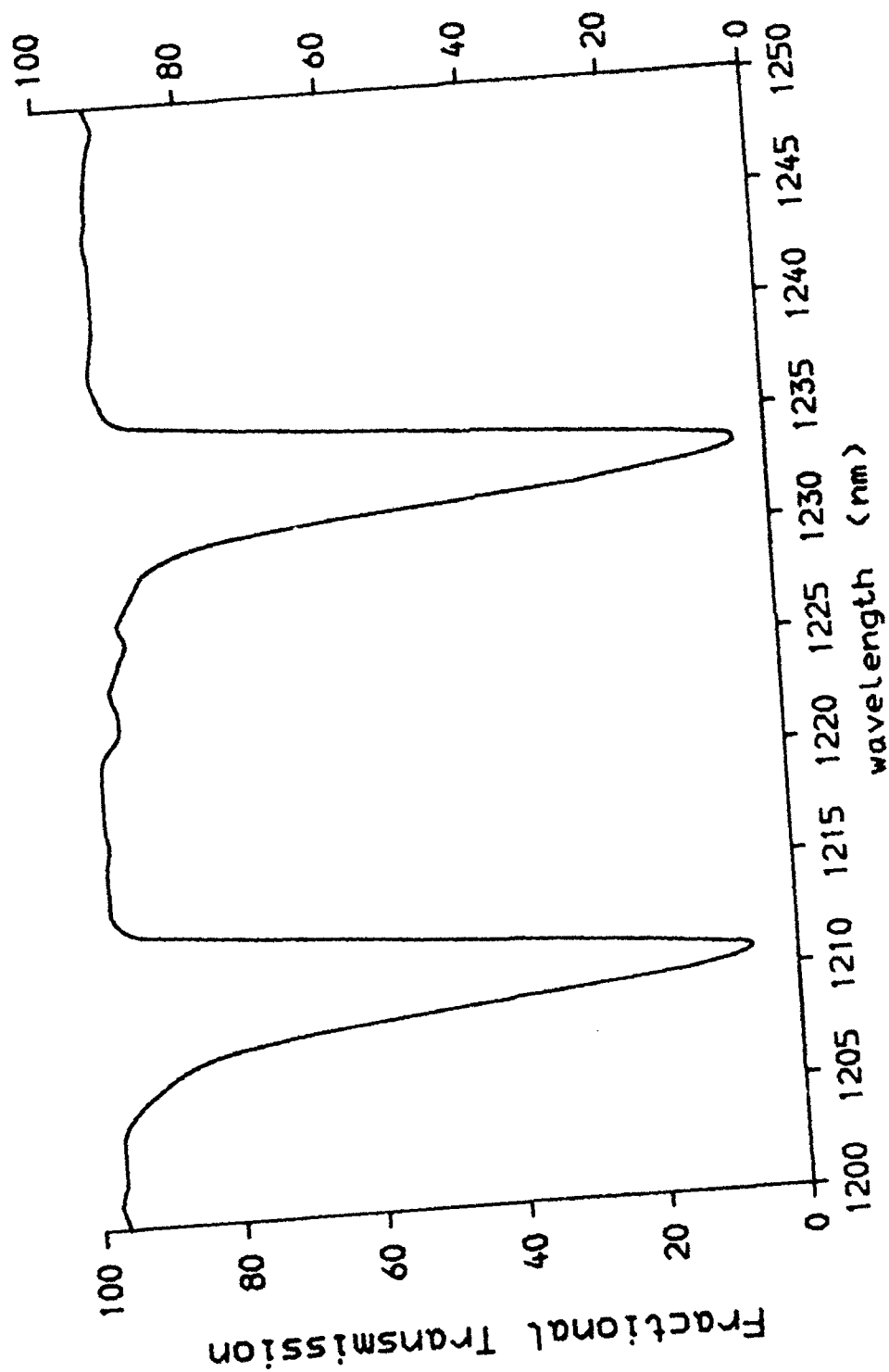


Fig. 22 Measured shift in the resonance wavelength of a 7.25  $\mu\text{m}$  thick BK7 overlay device as a function of  $\text{MgF}_2$  thickness



**Figure 23.** Wavelength response of a 20 $\mu$ m LiNbO<sub>3</sub> overlay device for TM polarisation

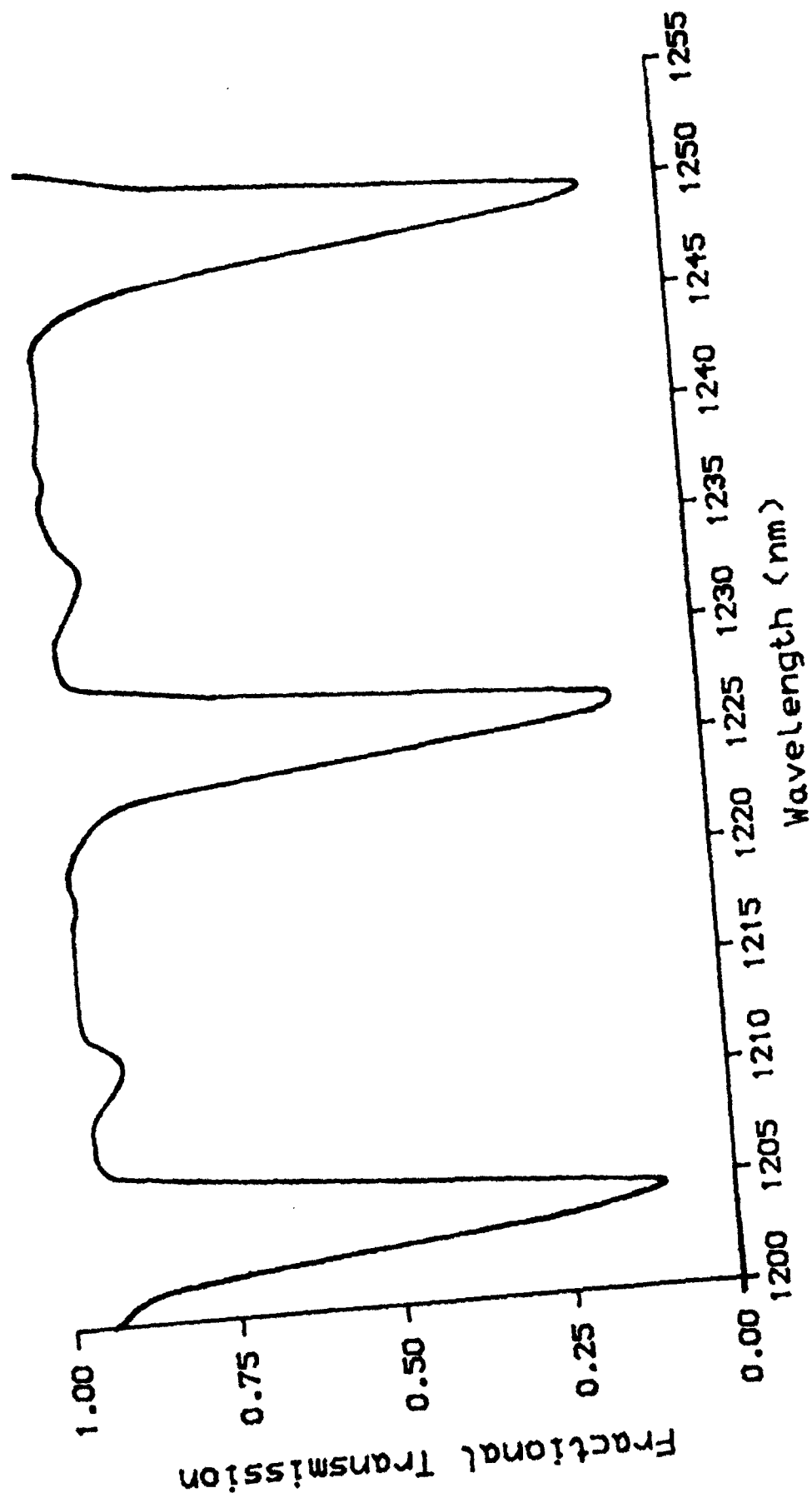
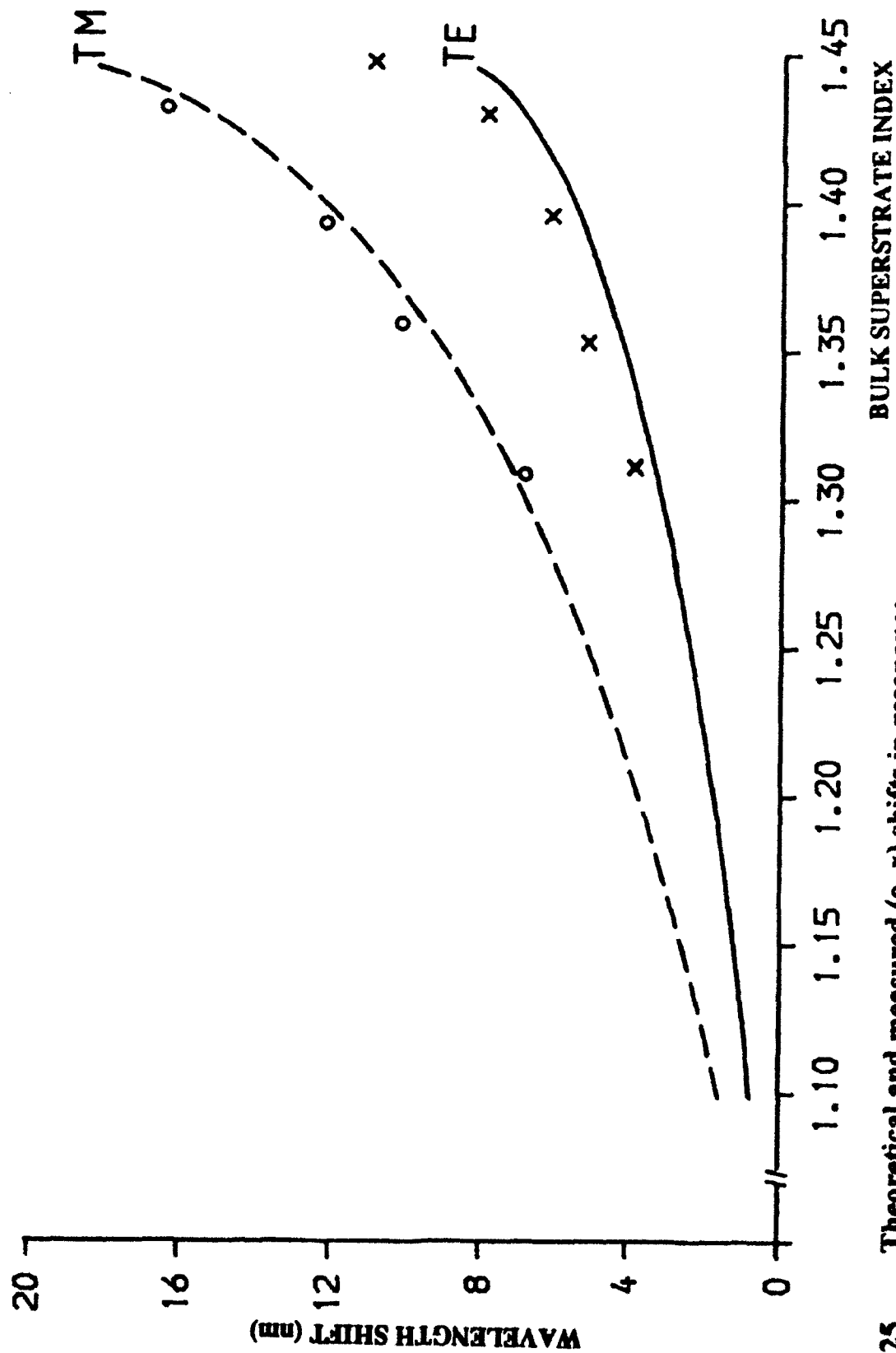


Figure 24. Wavelength response of a 20 $\mu$ m LiNbO<sub>3</sub> overlay device for TE polarisation





**Fig. 25** Theoretical and measured (o, x) shifts in resonance position versus superstrate index for a 20 $\mu$ m lithium niobate overlay device

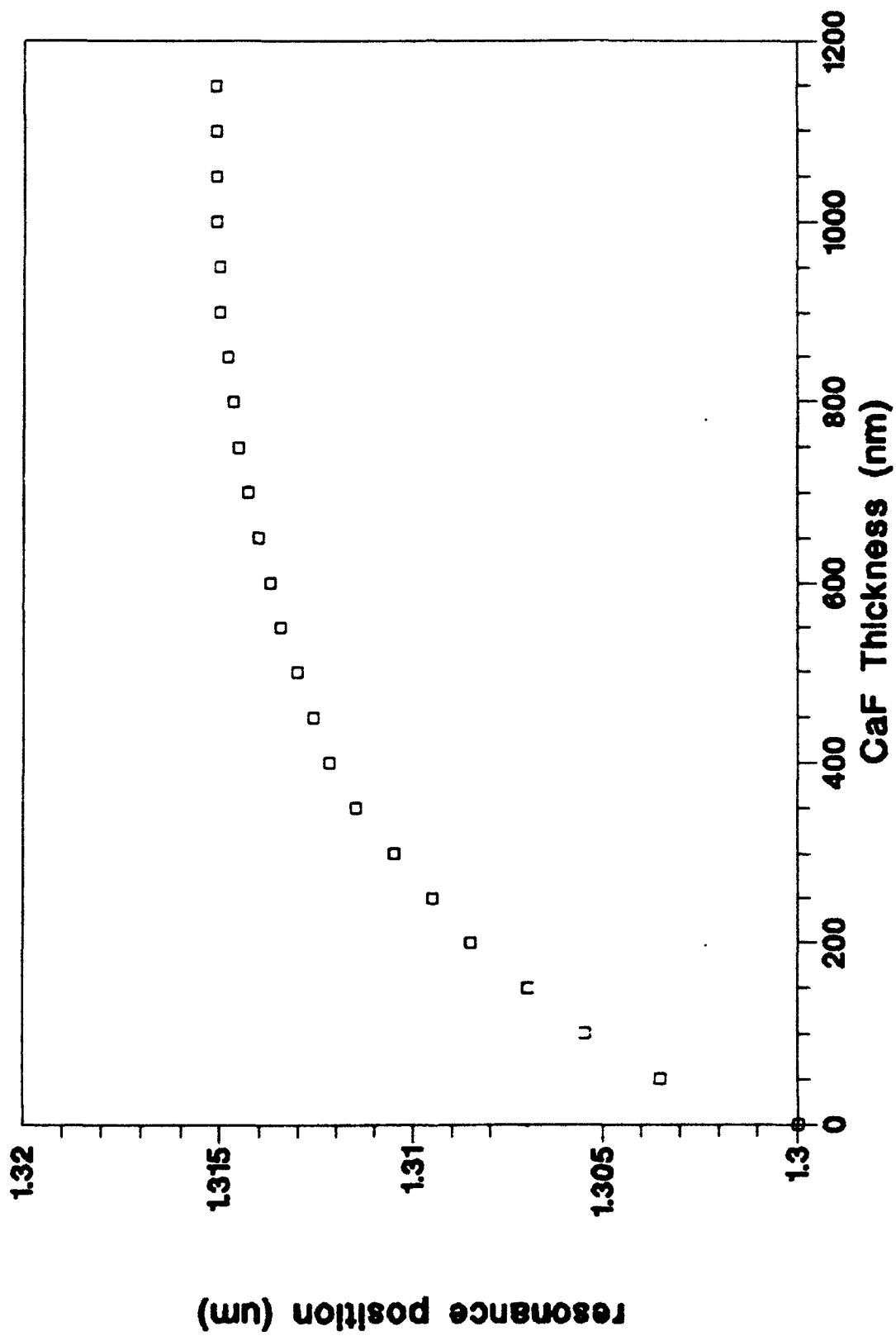


Fig. 26 Theoretical shift in resonance for 10um Lithium niobate overlay, TM polarisation

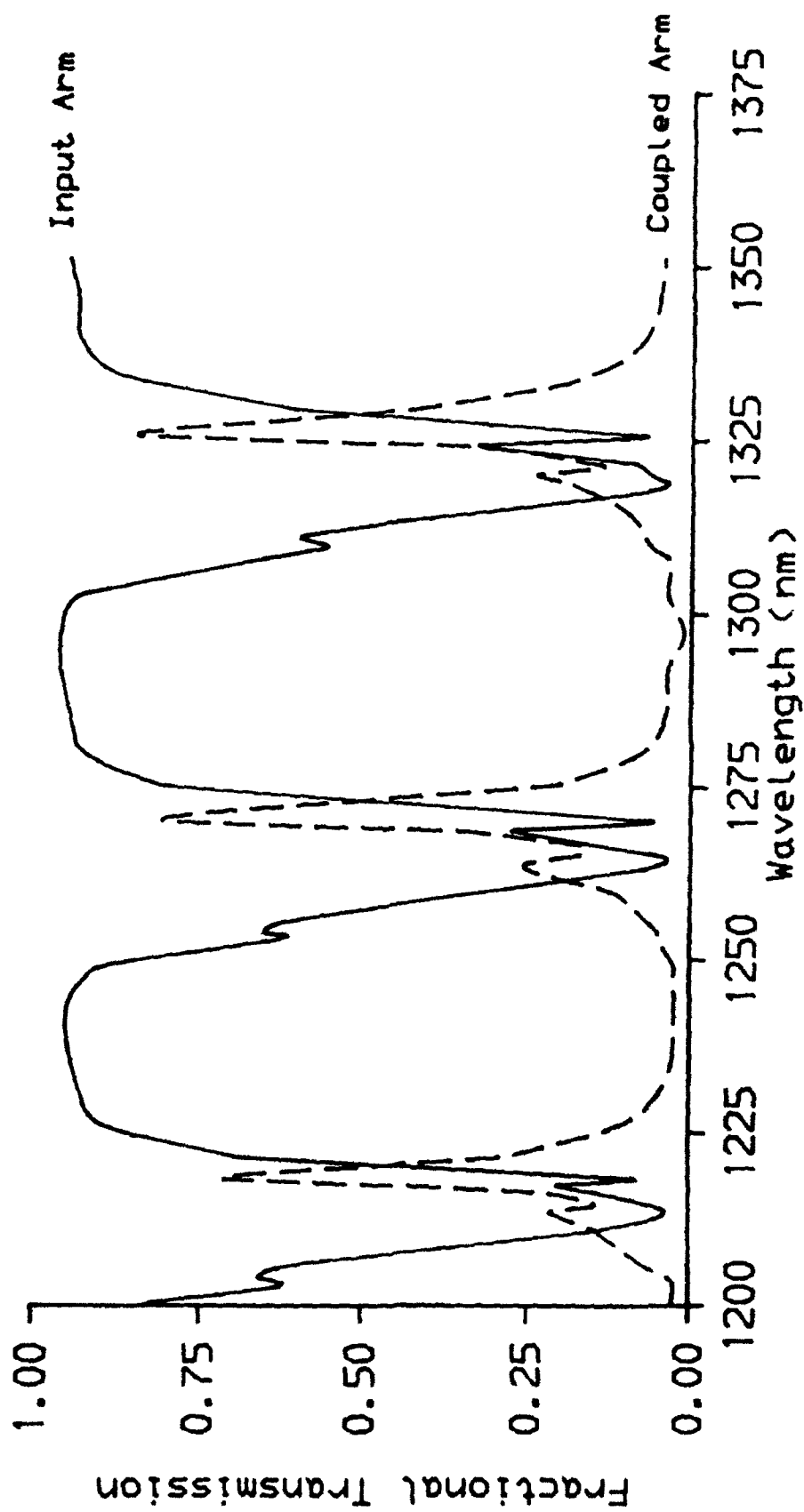


Fig. 27 Transmission characteristics between two side polished blocks with 10 $\mu$ m LiNbO<sub>3</sub> interlay: TM polarisation

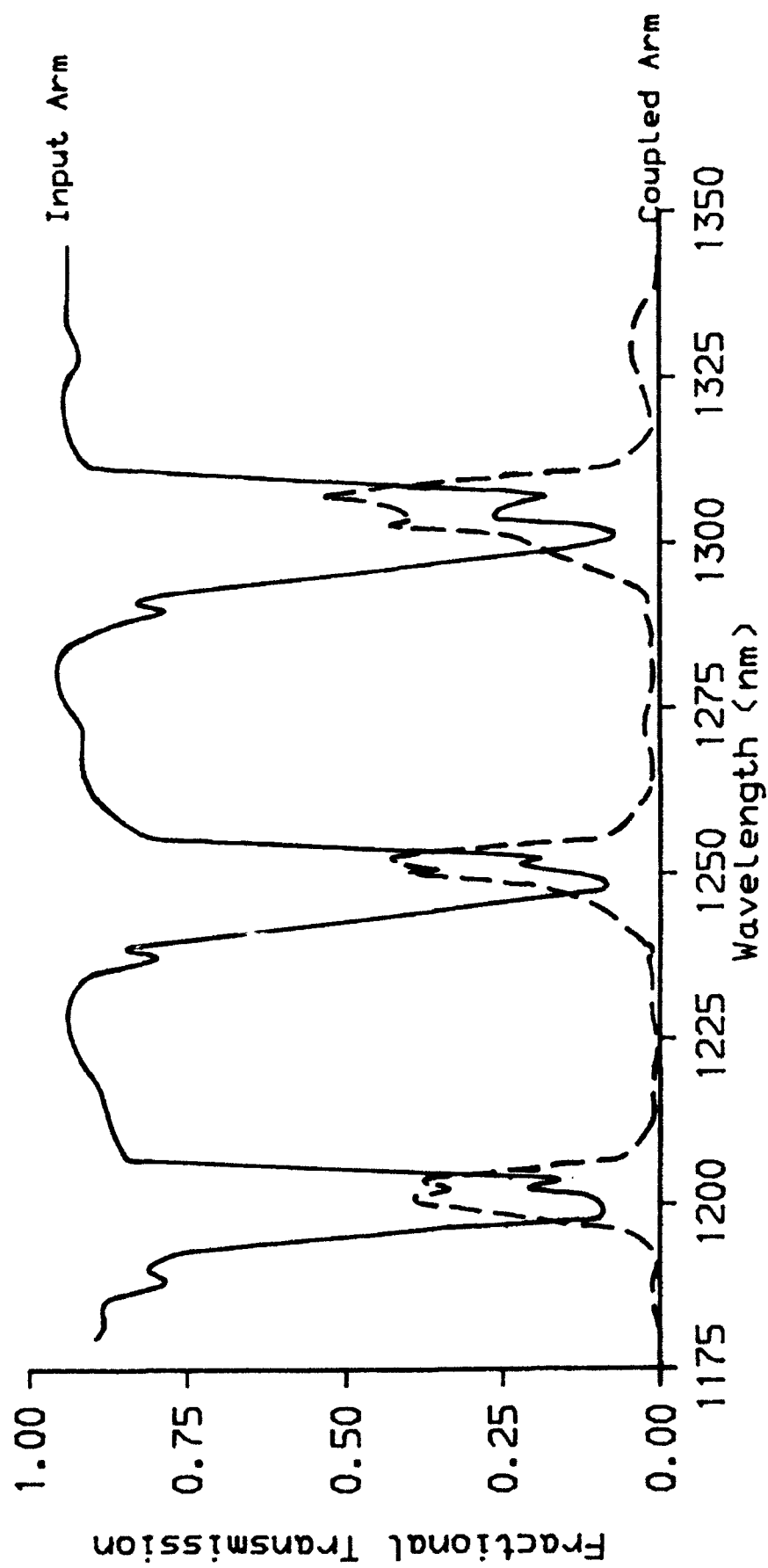
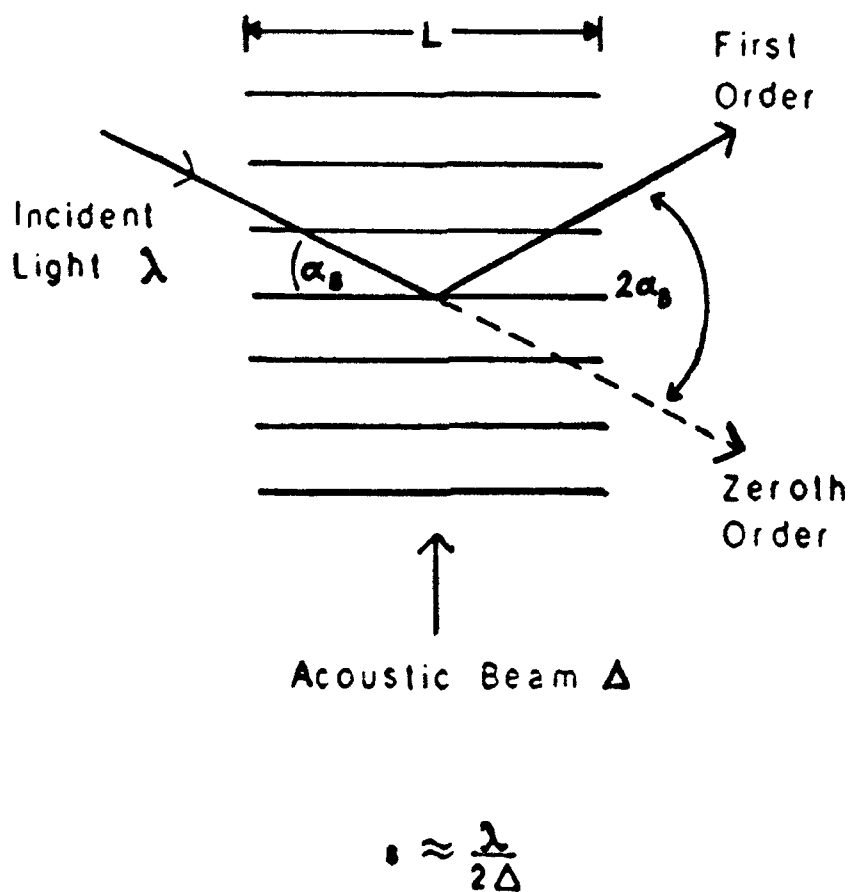
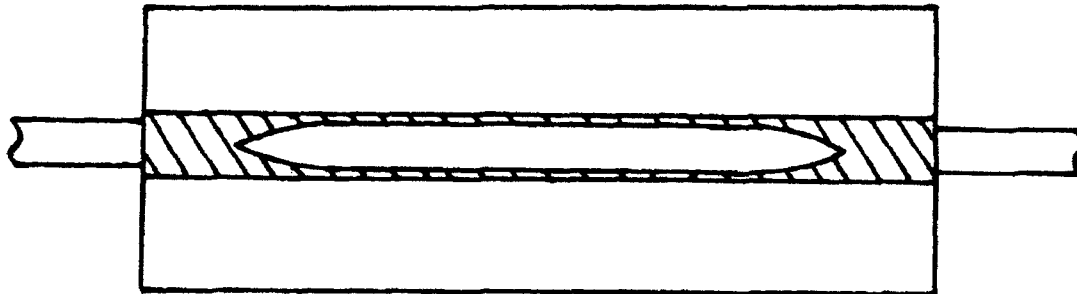


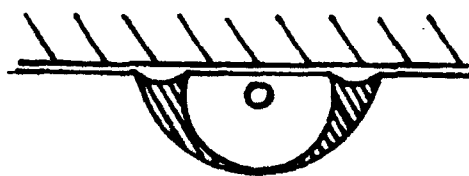
Fig. 28 Transmission characteristics between two side polished blocks with 10 $\mu$ m LiNbO<sub>3</sub> interlay: TE polarisation



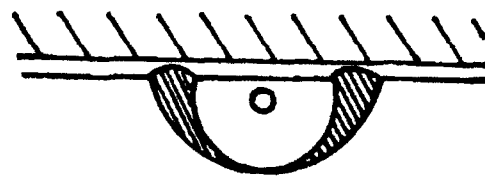
**Fig. 29** Acousto Optic Bragg Interaction process



Top view of fibre block showing polished fibre ellipse



(a) undercut



(b) proud

**Fig. 30**      **Effect of differential polishing rates on block flatness and glue line**

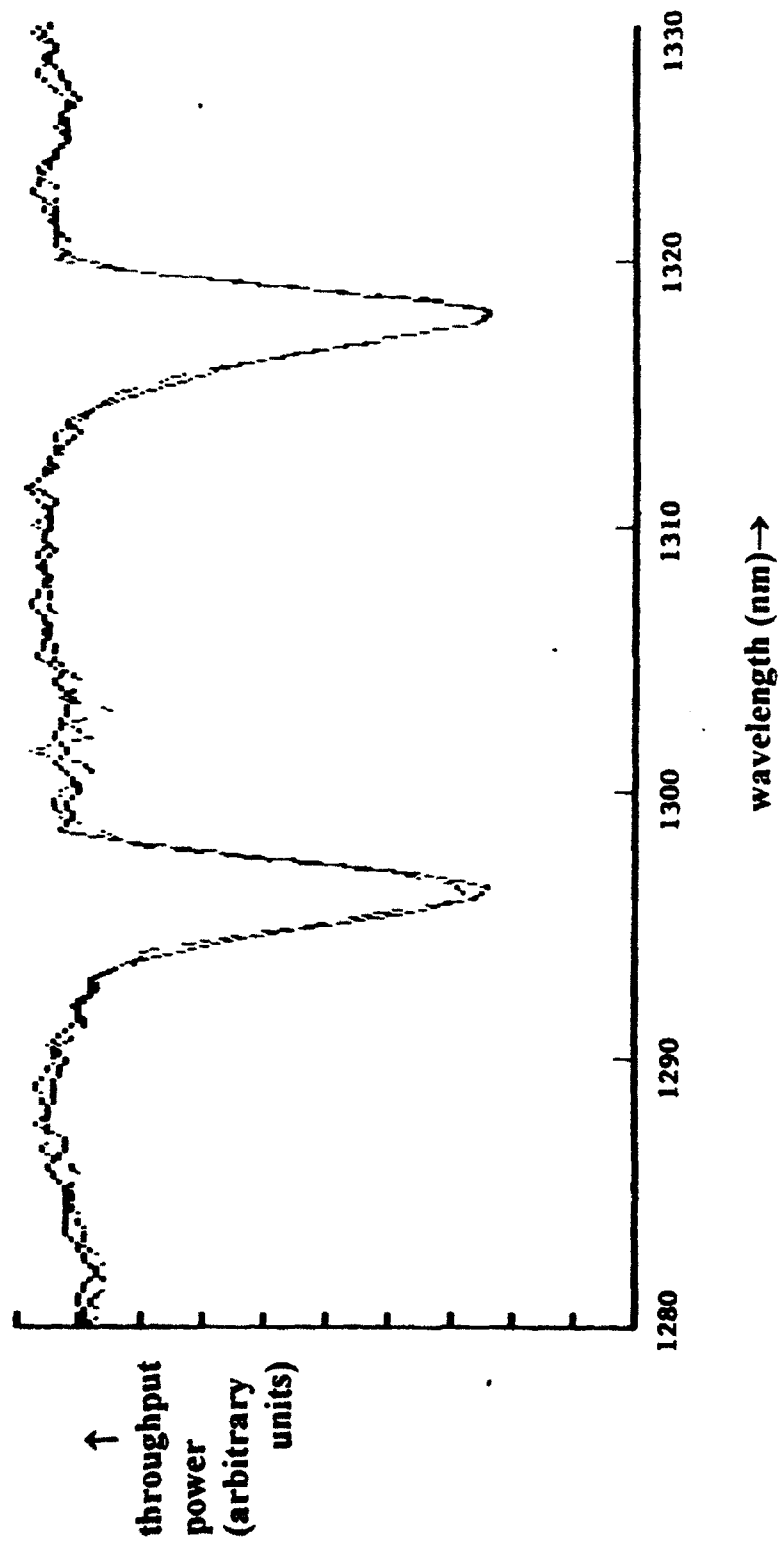


**Fig. 31** Wavelength transmission characteristics of a device having a 24 $\mu$ m thick lithium niobate overlay before and after application of 43.2MHz r.f. drive

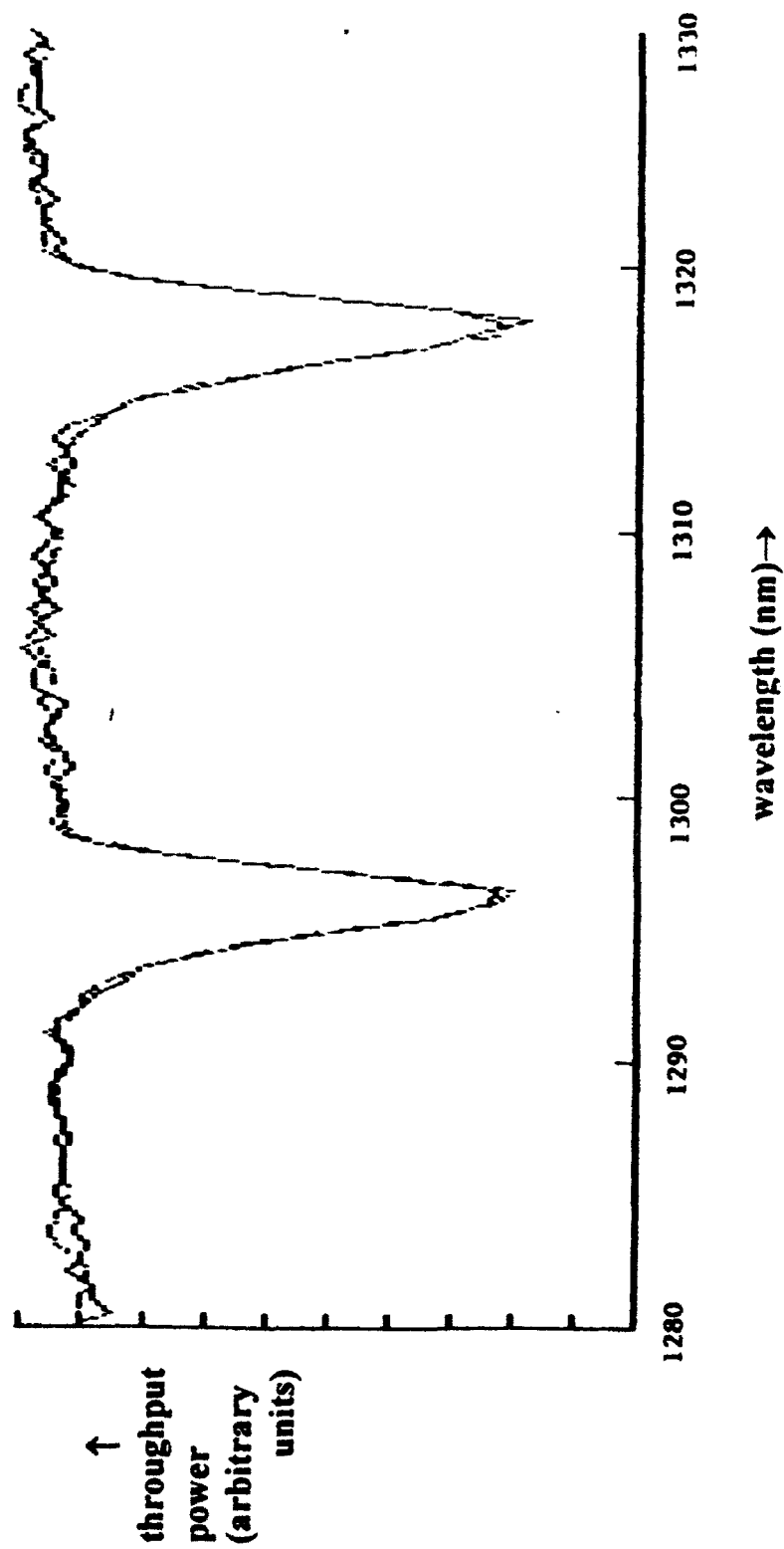


**Fig. 32** Wavelength transmission characteristics of a device having a 24 $\mu$ m thick lithium niobate overlay before and after application of 60MHz r.f. drive.



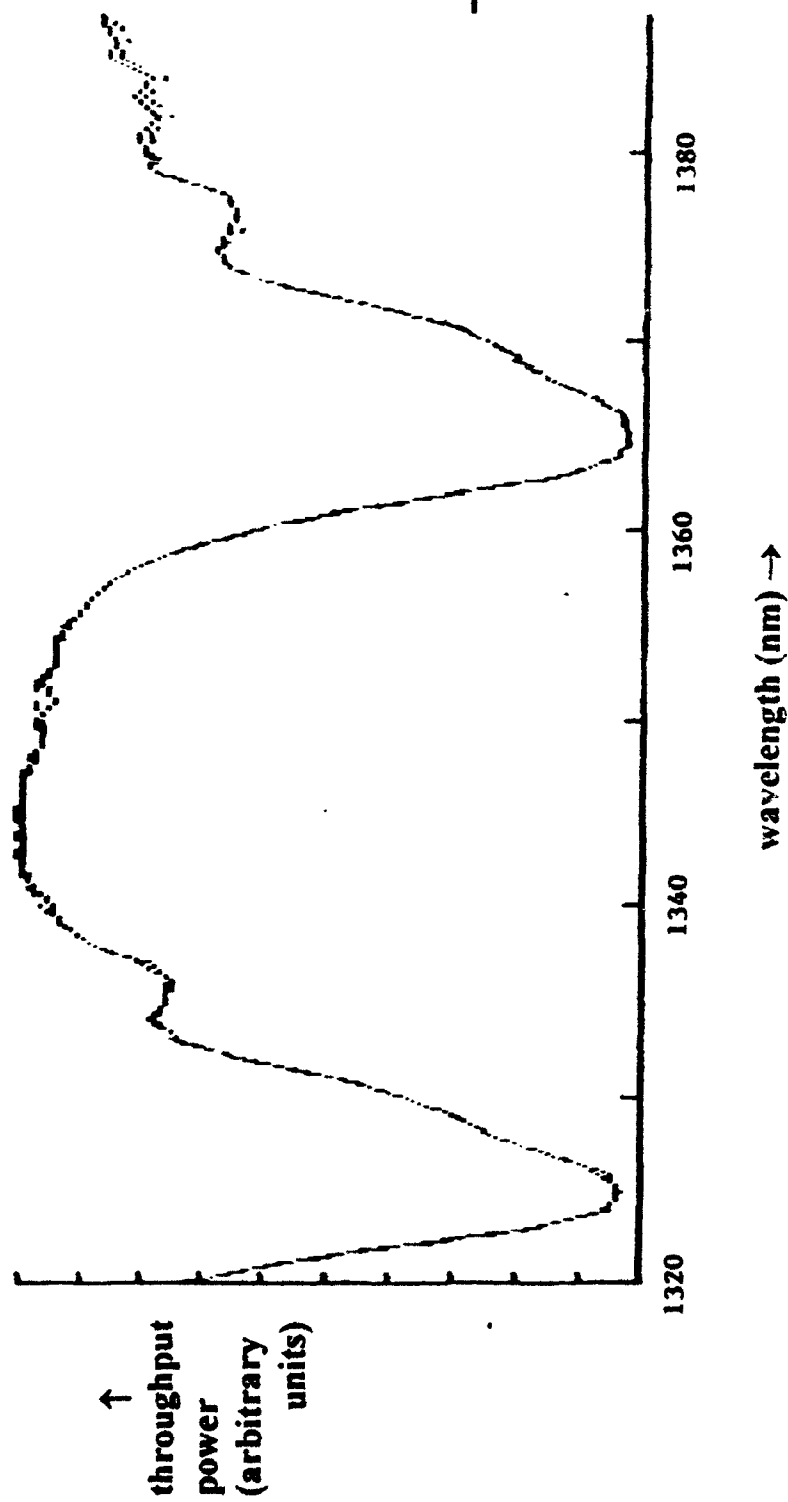


**Fig. 33** Wavelength transmission characteristics of a device having a 14 $\mu$ m thick lithium niobate overlay before and after application of 50V d.c. to the electrode structure (TM mode)

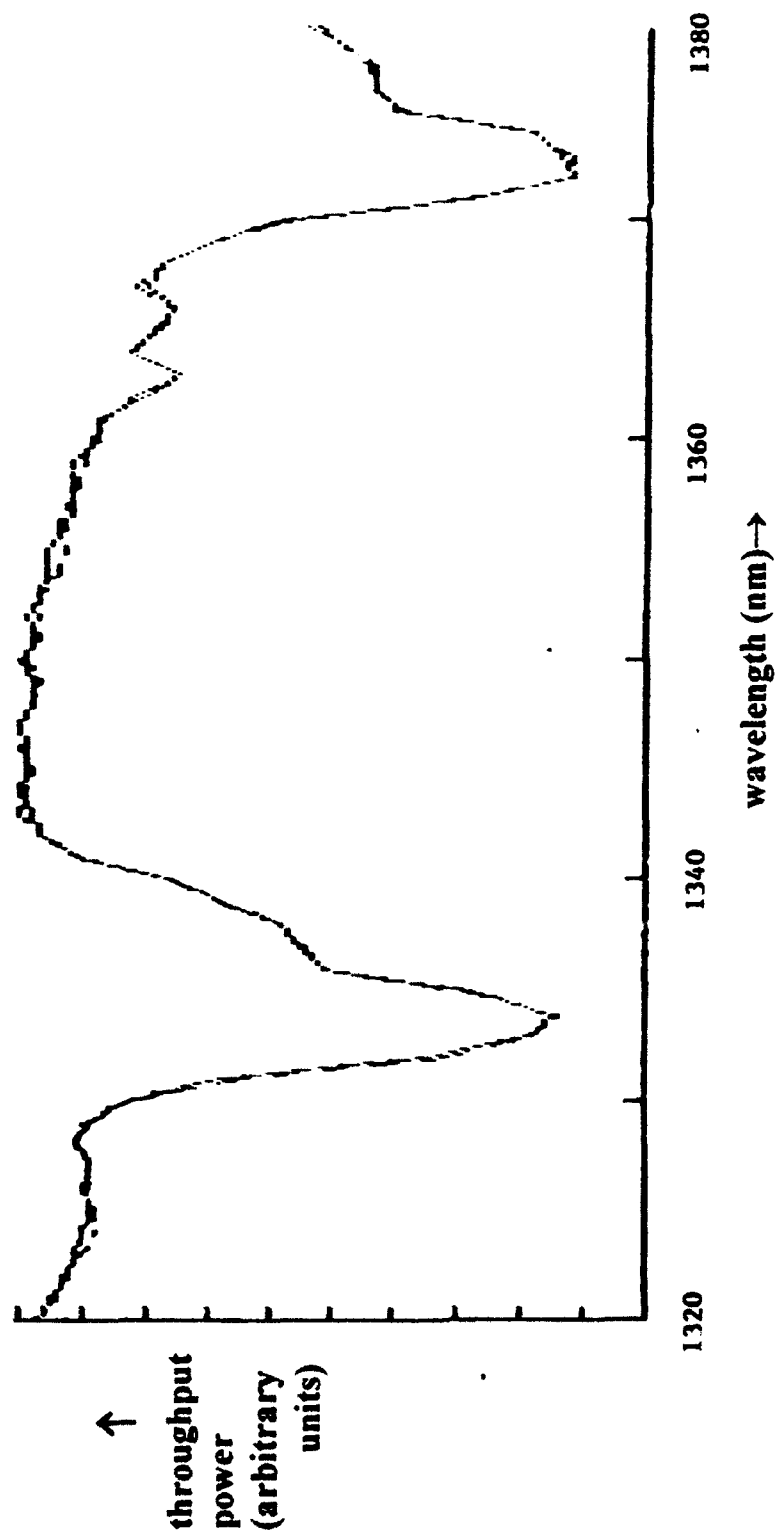


**Fig. 34** Wavelength transmission characteristics of a device having a 14 $\mu$ m thick lithium niobate overlay before and after application of 50V d.c. to the electrode structure (TE mode)

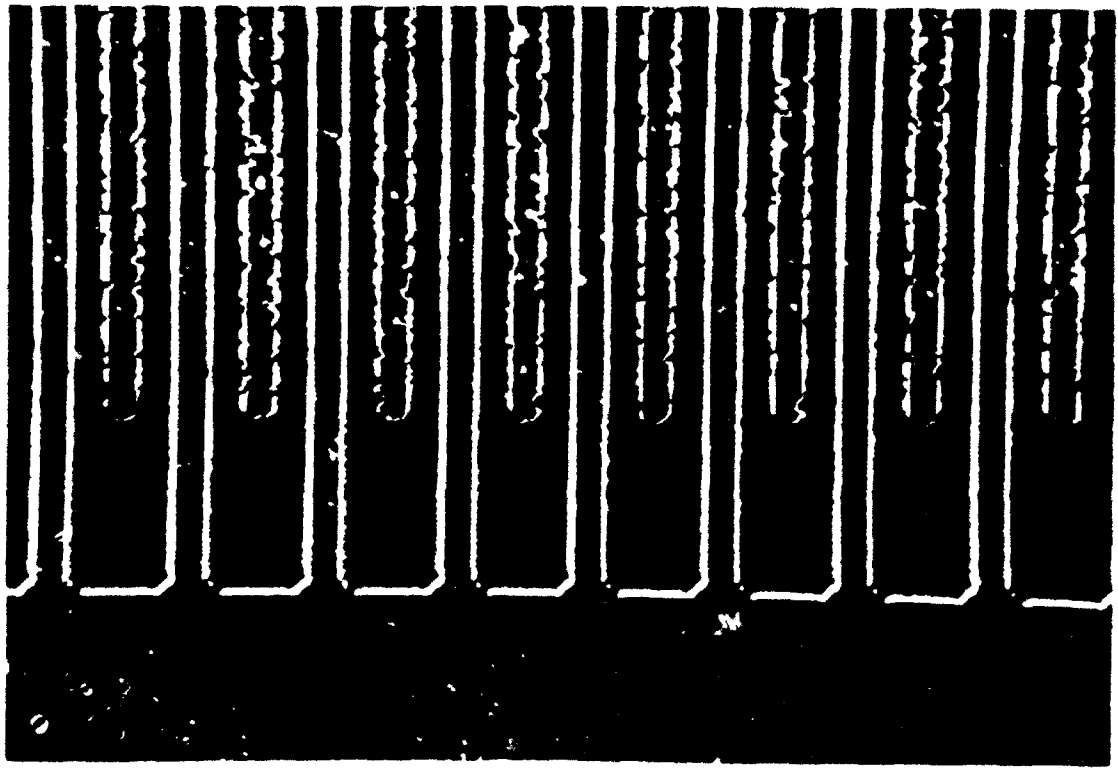


**Fig. 35**      Photograph showing damage to electrode structure caused by electrical breakdown

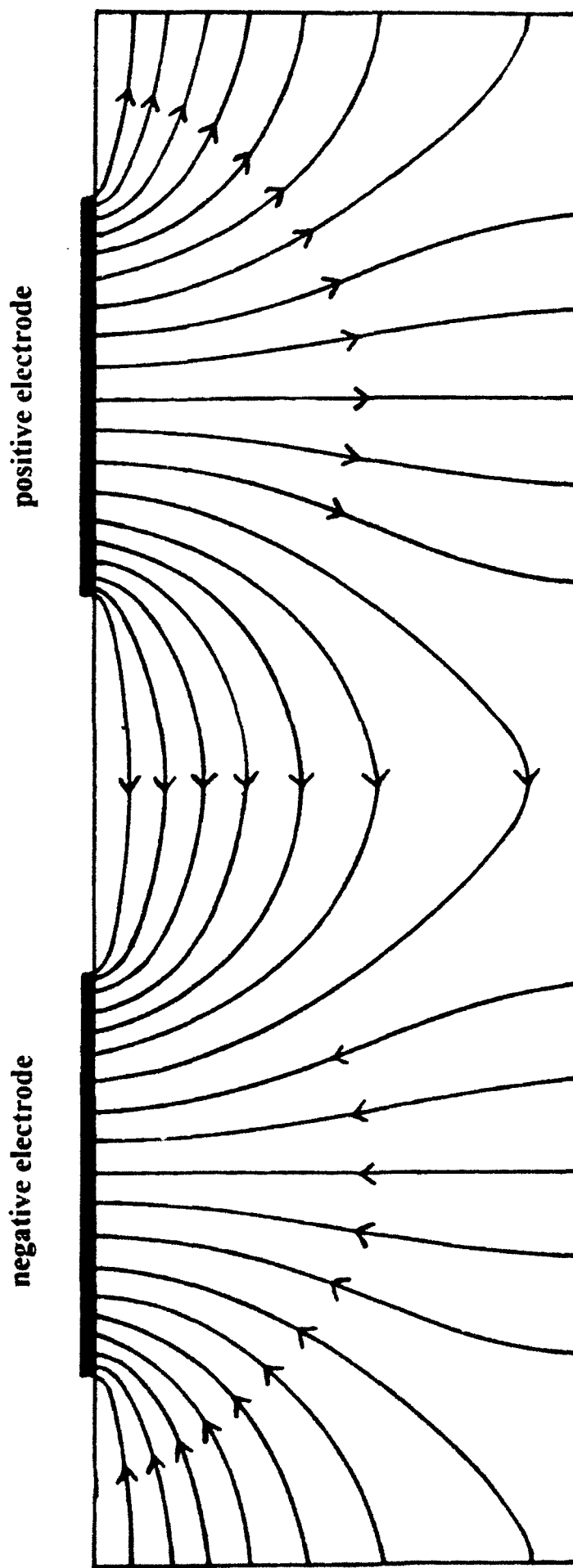


**Fig. 36** Diagram showing theoretical field distribution inside a lithium niobate overlay (niobate thickness  $25\mu\text{m}$ , electrode width and spacing both  $20\mu\text{m}$ )